PREPARATION AND PERFORMANCE ANALYSIS OF ACRYLONITRILE BASED NANOCOMPOSITE MEMBRANES FOR CHROMIUM (VI) REMOVAL FROM AQUEOUS SOLUTIONS

A THESIS SUBMITTED TO
THE GRADUATE SCHOOL OF NATURAL AND APPLIED SCIENCES
OF
MIDDLE EAST TECHNICAL UNIVERSITY

BY

SELÇUK BOZKIR

IN PARTIAL FULFILLMENT OF THE REQUIREMENTS
FOR
THE DEGREE OF MASTER OF SCIENCE
IN
POLYMER SCIENCE AND TECHNOLOGY

DECEMBER 2010

Approval of the thesis:

PREPARATION AND PERFORMANCE ANALYSIS OF ACRYLONITRILE BASED NANOCOMPOSITE MEMBRANES FOR CHROMIUM (VI) REMOVAL FROM AQUEOUS SOLUTIONS

submitted by **SELÇUK BOZKIR** in partial fulfillment of the requirements for the degree of **Master of Science in Polymer Science and Technology Department, Middle East Technical University** by,

Prof. Dr. Canan Özgen _____
Dean, Graduate School of **Natural and Applied Sciences**

Prof. Dr. Necati Özkan _____
Head of Department, **Polymer Science and Technology**

Prof. Dr. Ali Usanmaz _____
Supervisor, **Chemistry Dept., METU**

Asst. Prof. Dr. Mehmet Sankır _____
Co-Supervisor, Micro and Nanotech.Graduate Prog., TOBB-ETU

Examining Committee Members:

Prof. Dr. Duygu Kısakürek _____
Chemistry Dept., METU

Prof. Dr. Ali Usanmaz _____
Chemistry Dept., METU

Prof. Dr. Leyla Aras _____
Chemistry Dept., METU

Prof. Dr. Zuhal Küçükyavuz _____
Chemistry Dept., METU

Asst. Prof. Dr. Mehmet Sankır _____
Micro and Nanotech.Graduate Prog., TOBB-ETU

Date: 06.12.2010

I hereby declare that all information in this document has been obtained and presented in accordance with academic rules and ethical conduct. I also declare that, as required by these rules and conduct, I have fully cited and referenced all material and results that are not original to this work.

Name, Last name: SELÇUK BOZKIR

Signature:

ABSTRACT

PREPARATION AND PERFORMANCE ANALYSIS OF ACRYLONITRILE BASED NANOCOMPOSITE MEMBRANES FOR CHROMIUM (VI) REMOVAL FROM AQUEOUS SOLUTIONS

Bozkır, Selçuk

M.Sc., Department of Polymer Science and Technology

Supervisor: Prof. Dr. Ali Usanmaz

Co-Supervisor: Assist. Prof. Dr. Mehmet Sankır

December 2010, 90 pages

Acrylonitrile were copolymerized with 2-ethylhexyl acrylate and hexyl acrylate via one step emulsion polymerization using ammonium persulfate (initiator), 1-dodecanthiol (chain transfer agent) and DOWFAX 8390 (surfactant) in the presence of water at about 68 ^{0}C. Poly (acrylonitrile-2ethylhexyl acrylate) and poly (acrylonitrile-hexyl acrylate) copolymers with three different comonomer composition (8, 12 and 16 molar percent) were prepared. FTIR and ^{1}H-NMR were used in order to clarify the chemical structure of copolymers. The comonomer amount incorporated into copolymers was determined by using ^{1}H-NMR spectra. The thermal behavior of copolymers was determined by DSC and TGA. Molecular weights of copolymers were determined by intrinsic viscosity (IV) measurements. IV measurements revealed that both poly (acrylonitrile-2ethylhexyl acrylate) and poly (acrylonitrile-hexyl acrylate) have sufficient molecular weight to form nanoporous filtration membranes.

Nanoporous filtration membranes were prepared and tested for chromium (IV) removal. It was observed that chromium (VI) rejections of nanoporous filtration membrane were highly dependent on the concentration and the pH of the solutions. Almost complete removal (99, 9 percent Cr (VI)) rejection was achieved at pHs 2, 5 and 7 for solution containing 50 ppm, chromium (VI) with permeate flux within a range from 177 to 150 L/m2h at 689.5 kPa. Also, chemical structure, swelling ratios, sheet resistivity and fracture morphologies of the nanoporous filtration membrane were studied. It should be noted that the nanoporous filtration membranes were fouling resistant.

Keywords: Acrylonitrile, Emulsion Polymerization, Removal of Chromium ion, Nanoporous filtration membranes

ÖZ

KROM (VI)'YI SULU ÇÖZELTILERDEN UZAKLAŞTIRMAK IÇIN AKRILONITRILE TABANLI NANOKOMPOSIT MEMBRANLARININ HAZIRLANMASI VE TEST EDILMESI

Bozkır, Selçuk

Yüksek Lisans, Polimer Bilimi ve Teknolojisi Bölümü

Tez Yöneticisi: Prof. Dr. Ali Usanmaz

Ortak Tez Yöneticisi : Yrd. Doç. Dr. Mehmet Sankır

Aralık 2010, 90 sayfa

Akrilonitril, 2-etilheksil akrilat ve heksil akrilat ile tek adımlı emülsiyon polimerizasyon tekniği ile kopolimerleştirilmiştir, amonyum persülfat (başlatıcı), 1-dodekantiyol (zincir transfer maddesi) ve DOWFAX 8390 (surfactant) kullanarak yaklaşık 68 ^{0}C lik su ortamında hazırlandı. Poli (akrilonitril-2etilheksil akrilat) ve poli(akrilonitril-heksil akrilat) kopolimerleri üç değişik komonomer komposiyonunda (8, 12 ve 16 mol yüzdesinde) sentezlendi ve karakterize edildi. Kopolimerlerin kimyasal yapılarını doğrulamak için FTIR ve ^{1}H-NMR karakterizasyon metodları uygulandı. Kopolimer içindeki komonomer komposizyon miktarları ^{1}H-NMR ile belirlendi. Kopolimerlerin termal davranışları DSC ve TGA yöntemleriyle araştırıldı. Kopolimerlerin molekül kütleleri IV ölçümleri ile belirlendi ve IV ölçümleri Poli (akrilonitril-2etilheksil akrilat) ve poli (akrilonitril-heksil akrilat) kopolimerlerinin her ikisinin de nano gözenekli filtrasyon membran oluşturmak için yeterli olduğunu göstermiştir.

Nano gözenekli filtrasyon membranları hazırlandı ve krom (VI) yı sulu çözeltilerden uzaklaştırmak için test edildi. Krom (VI) pH'ı 2, 5 ve 7 olan 50 ppm krom (VI) içeren solüsyonlarda kalıcı fluksları 177-150 L/m^2h aralığında değişen şekilde ve 689.5 kPa basınçda yaklaşık olarak tamamı sudan uzaklaştırılacak şekilde başarılı şekilde gerçekleşti. Ayrıca, nano gözenekli filtrasyon membranlarının kimyasal yapıları, şişme oranları, sheet dayanıklılıkları ve kesit morfolojileri çalışıldı. Özellikle belirtmek gerekir ki nano gözekli membranlar fouling dayanıklıdır.

Anahtar Kelimeler: Akrilonitril, Emülsiyon Polimerizasyonu, Krom İyonunun Süzülmesi, Nano gözenekli filtrasyon membranları

To My Family

ACKNOWLEDGEMENTS

I would like to express my sincere thanks and gratitude to my advisors, Prof. Dr. Ali USANMAZ, for his valuable guidance, support, patience and direction leading me to the better throughout my graduate school years here at Middle East Technical University. I also thank him for teaching me the way of positive thinking and how to fulfill my potential.

I would like to thank my co-advisor Asst. Prof. Dr. Mehmet Sankır who taught to me everything related to polymer and he has been tireless advisor during my education. I am also grateful him for supporting me morally throughout the thesis. Without his help, this work would not have been possible.

I would like to thank my coworkers for all their help through the past few years including Bengi Aran, Bahadır Doğan, Tamer Tezel, and Levent Semiz for their help and understanding. Additionaly, my thanks go to Bengi Aran for supporting me during my lessons and helped me anytime I needed.

Thanks also to Asst. Prof. Dr. Nurdan D. Sankır for her supporting, understanding and being so helpful any times of need.

TUBITAK is gratefully acknowledged for the financial support via grant no 108T099.

Finally, I wish to express my deep appreciation to my family, for being always so supportive and having an understanding. Without their courage and love, this work could not be accomplished

TABLE OF CONTENTS

LIST OF TABLES

TABLES

LIST OF FIGURES

FIGURES

CHAPTER 1

INTRODUCTION

1.1 Acrylonitrile

Acrylonitrile (also called acrylic acid nitrile, propylene nitrile, vinyl cyanide, propenoic acid nitrile) is a monomer with a molecular formula of C_3H_3N which contains carbon-carbon double bond conjugated with a nitrile group. The presence of the nitrogen heteroatom allows the acrylonitrile to become a polar molecule so that there is a partial shift in the bonding towards the more electronegative nitrogen atom. The chemical structure of the acrylonitrile monomer can be seen in Figure 1 and the physical properties are given in Table 1.

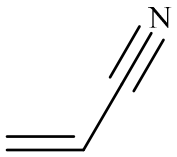

Figure 1.1 Structure of Acrylonitrile

The polymerization of acrylonitrile takes place through the vinyl group by chain polymerization; as a result the polymer backbone is a vinyl type polymer.

Table 1.1 Physical Properties of Acrylonitrile [1]

Appearance/Odor	Clear, colorless liquid with fainty pungent odor
Boiling Point, ^{O}C	77.3
Freezing Point, ^{O}C	-83.5
Flash Point, ^{O}C	0
Density, 20 ^{O}C, g/cm^3	0.806
Vapor Density (air=1)	1.8

Hydroquinone inhibits the polymerization of acrylonitrile so when the medium is free from hydroquinone inhibitors it can be polymerized readily especially when exposed to light. Free radicals, redox catalysts or bases can initiate the polymerization and the polymerization can be carried out in liquid, solid or gas phase. Moreover, liquid phase polymerization systems such as solution and emulsion polymerization are suitable for the production of homo and copolymer of acrylonitrile. Acrylonitrile is mainly used for the production of several industrially important polymers such as acrylic fiber, acrylonitrile-butadiene-styrene (ABS) resins, nitrile rubbers, elastomers, styrene-acrylonitrile (SAN) resins and polyacrylonitrile [1].

1.2 Hexyl acrylate and 2-ethylhexyl acrylate

Acrylates are the class of ester compound has general molecular formula shown in Figure 1.2

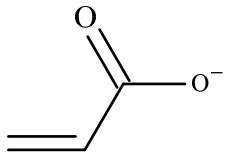

Figure 1.2 General formulas of acrylate esters

Although copolymers of acrylates esters are used in several different areas, homopolymer are preferred only in a few areas of application. For the production of copolymers the following comonomers are commonly used; methacrylate, styrene, acrylonitrile, vinyl chloride, vinyldiene chloride and butadiene. A carbonyl group adjacent to a vinyl group makes the polymerization of acrylates easier. The production of acrylates polymers is achieved by radical polymerization and the polymerization is initiated by photochemically or an azo starter or by electron beams. An emulsion polymerization system is the most preferred system by industry in the preparation of polylacrylates. Solution and bulk polymerization are also used however bulk polymerization is only performed on a small scale as compared to solution and emulsion polymerization [2].

In this thesis, hexyl acrylate and 2-ethylhexyl acrylate were used to prepare copolymers of acrylonitrile. Their chemical structure can be seen in figure 3 and 4 and their physical properties are given in table 2 and 3.

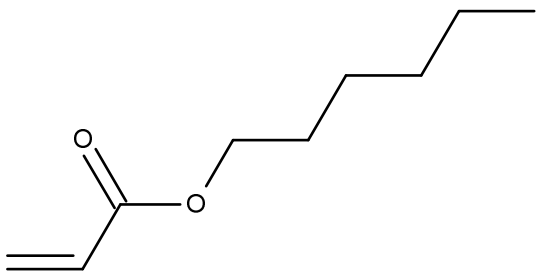

Figure 1.3 Chemical Structure of hexyl acrylate.

The polymerization of hexyl acrylate takes place through the vinyl group by chain polymerization; as a result the polymer backbone is a vinyl type polymer.

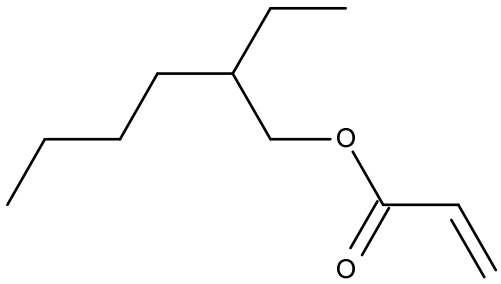

Figure 1.4 Chemical Structure of 2-ethylhexyl acrylate

The polymerization of 2-ethylhexyl acrylate takes place through the vinyl group by chain polymerization; as a result the polymer backbone is a vinyl type polymer.

Table 1.2 Physical Properties of hexyl acrylate [2]

Appearance	Clear
Boiling Point, 2.5 kPa, ^{O}C	89
Freezing Point, ^{O}C	-46
Solubility in water, 25 ^{O}C g/100cm^3)	0.04
Solubility in water, 80 ^{O}C g/100cm^3)	0.08
Density, ^{O}C	0.88

Table 1.3 Physical Properties of 2-ethylhexyl acrylate [2]

Appearance	Clear
Boiling Point, 101.3 kPa, ^{O}C	217
Solubility in water, 25 ^{O}C (g/100cm^3)	0.04
Solubility in water, 80 ^{O}C g/100cm^3)	0.04
Density, ^{O}C	0.88

1.3 Polymerization of Acrylonitrile

Emulsion polymerization is the process for producing polyacrylonitrile-co-polyacrylates copolymers. Emulsion polymerization is a non-homogeneous method that is composed of a water soluble initiator, water insoluble monomer and a micelle forming surfactant. High molecular weight polymers can be obtained in a short time because of the high polymerization rates. Aqueous medium reduces the viscosity of medium and the heat from polymerization can be easily removed [2, 3].

1.3.1 Emulsion Polymerization

Emulsion polymerization is a widely used technique that is employed in the production of several types of commercial polymers. In order to synthesize a polymer by this method, the monomers of a polymer must have at least water solubility. Polymerization of monomers such as vinyl acetate, chloroprene, ethylene and copolymerization of various acrylates and copolymerization of styrene with butadiene and acrylonitrile are achieved by emulsion polymerization. Methacrylates, vinyl chloride, acrylamide, and some fluorinated ethylenes are also polymerized by this method [4]. There are many areas where emulsion polymers

can be used, such as synthetic rubbers, thermoplastics, coatings, adhesives, binders, rheological modifiers, plastic pigments, standards for the calibration of instruments, immunodiagnosis tests, polymeric supports for the purification of polymers and drug delivery system, etc [5].

Batch, semi-batch and continuous are three types of processes that are used in emulsion polymerization. Batch emulsion polymerization process is the preferred in laboratory in order to produce new latex particles, to obtain new kinetic data for process development and to redesign a reactor [5]. All ingredients are mixed at the beginning of the reaction and when the initiator begins to dissociate into its radicals at proper temperature, polymerization takes place and latex particles start to grow in the batch process. The semi-batch emulsion polymerization process differs from the batch process only in that one or more ingredients continuously added. The order with which the ingredients are added the polymerization medium affects the particles nucleation and the growth of the polymer. In the continuous process, while ingredients are added continuously by a series of tanks into the polymerization medium, the formed latex particles are removed simultaneously [3]. The majority of commercial polymers are produced by the semi-batch or the continuous process because it is easy to control the temperature and the large scale heat transfer of the polymerization reactor [5]. The continuous emulsion process also has some advantages over the batch and the semi-batch processes, due to the high production rate, the steady heat removal and the uniform quality of latexes [3].

Emulsion polymerization is a heterogeneous free radical polymerization method that includes the emulsification of a hydrophilic monomer or a mixture of monomers in an aqueous phase and stabilization of this system with a surfactant. A typical emulsion polymerization medium contains monomer, water, surfactant and a water soluble initiator. The addition of the surfactant at the beginning of the reaction facilitates the formation of emulsified monomer droplets (5-10 μm in diameter, 10^{12}-10^{14} dm^{-3}) dispersed in the continuous aqueous phase. The necessity of this system is the formation of micelles next to the stabilized monomer droplets.

Most of the monomer remains as giant monomer droplets and only if the concentration of the surfactant exceeds its critical micelle concentration, will the monomer swollen micelles appear in the reaction system. Then, the water soluble initiator starts the polymerization in micelles, which are then converted to a product known as latex. Latex can be defined as a colloidal dispersion of polymer particles in an aqueous phase [5].

The most commonly used water soluble initiators are peroxo compounds such as alkali persulfates, ammonium persulfate or hydrogen persulfates and polymerization generally takes place between reaction temperatures of 50 and 85 ^{O}C. Moreover, a redox system can be preferred to initiate the polymerization, but the reaction temperature should be below 50 ^{O}C [2].

Water is the key ingredient for both suspension and emulsion polymerization. It acts as a heat sink or a heat transfer agent and lowers the viscosity of the medium. Water has additional functions in emulsion polymerization such as it acts as a medium for the decomposition of the initiator and the oligomer formation, as a medium for the transfer of the monomer from droplets to particles and as the medium for the dynamic exchange of the surfactant between phases [3].

A surfactant can be defined as a molecule with both hydrophilic and hydrophobic segments. These segments provide sites for the nucleation of the particles and also facilitate to stabilize the growing colloidal particles in the water medium. Anionic surfactants are commonly preferred in emulsion polymerization methods. However, if synthesized polymer is used for a specific application such as for forming cationically charged latex particles in paper coatings and asphalt additives, cationic surfactants are preferred and for controlling latex particle morphology and for enchanting post polymerization colloidal stability against mechanical shear and freezing, non ionic surfactants are preferred. Moreover, if polymerization requires some special advantages, a reactive surfactant should be used. For example, these types of surfactant react chemically with the surface of the particles to reduce

desorption during the film formation and reduce the water sensitivity of the latex films [3].

Electrolytes and chain transfer agents are the other components that can be used during polymerization. Electrolytes can control the pH of the medium and ensure the efficiency of the initiator. For example, above pH 6 and temperature of 50^{O}C, the dissociation of persulfate initiator can be seen in the following reaction;

$$S_2O_8^{2-} \rightarrow 2SO_4^- \cdot$$
$$H_2O + SO_4^- \cdot \rightarrow HSO_4^- + OH \cdot$$

Since the formation of HSO_4^- lowers the pH of the medium, it is necessary to add a buffer in order to control the pH. Moreover, the reasons why chain transfer agents are used in to emulsion polymerization are to control the molecular weight of the product and to obtain polymers with a desired molecular weight. A mercaptan can be used as a chain-transfer agent to control the polymer molecular weight. [3].

1.3.1 Qualitive aspect of emulsion polymerization

The emulsifier or surfactant is a molecule which is composed of a hydrophobic tail with a polar head group and the head group may be ionic or neutral. Upon introduction of the surfactant into the polymerization medium (water), when the concentration of the surfactant molecules go beyond its critical micelles concentration (CMC), the surfactant molecules have a tendency to form aggregates spontaneously, that is, surfactant molecules will arrange themselves into organized small colloidal cluster molecules , also called micelles. Micelle formation is followed by the transformation of the aqueous phase into the colloidal phase and in order to ensure this, the free energy of the medium must be lowered by an abrupt decrease in the surface of the solution. Typical micelles have a spherical or a rodlike shape depending on surfactant and have a concentration with a dimensions

range between 2-10nm and each micelle contains 50-150 surfactant molecules. The surfactant molecules in the micelles arrange themselves in the following way; hydrocarbon tails attaches to the interior of the micelles and their polar head stays in the aqueous phase [4].

A water soluble initiator generates free radicals in the aqueous phase. Polymerization starts with the capturing of free radicals by micelles. However, free radicals are too hydrophilic to penetrate into the micelles to start polymerization. Therefore, monomer molecules dissolved in a continuous aqueous phase are polymerized by free radicals. This makes the free radicals more hydrophobic when the chain lengths of the oligomeric radicals are long enough. Thus, they show a tendency to enter the monomer-swollen micelles and the propagation reaction continues with the monomer molecules within the micelles. Finally, the monomer swollen micelles are converted into the particles nuclei. The colloidal stability of the growing particle nuclei is ensured by using micelles that do not participate nucleation, which disband and are used as a surfactant supply [5].

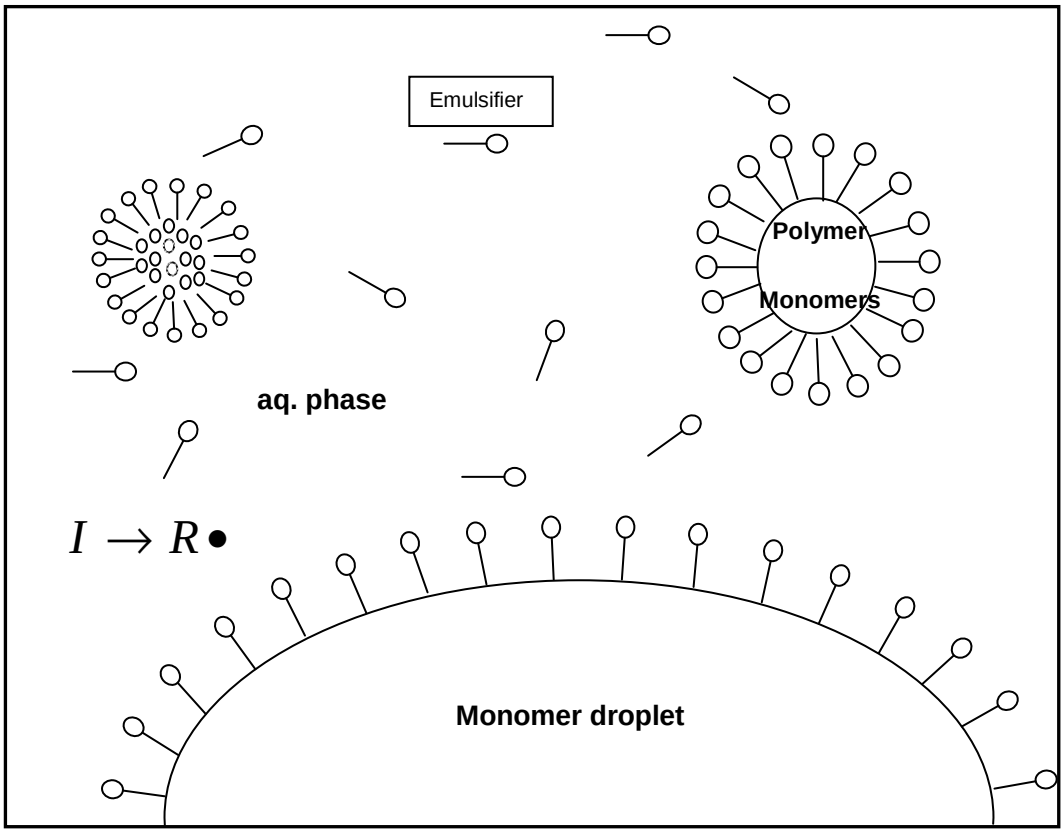

Figure 1.5 Schematic representation of an emulsion polymerization system [4].

1.3.2 Progress of emulsion polymerization

As stated in the qualitative aspect of the emulsion polymerization, particle nucleation starts in Interval I and polymerization rate increases as the number of particle increases over time. While polymerization is proceeded in the particle nuclei, which contains both polymer and monomers, in order to maintain the stability of the growing particles they absorb more surfactant from the solution. Thus, the concentration of surfactant in the solution falls below its critical micelles concentration at a specific time. During this period of time, micelles in which particle nucleation does not occur are disbanded and used as a surfactant supply. Before the end of interval I or very early in interval II absorption of all or almost all of the surfactant in the system by the polymer particles will take place. The particle

nucleation step ends immediately after exhaustion of all the micelles .Interval I is usually the shortest of the three intervals and 2-15% conversion takes place during this interval. Moreover, it can be observed that interval I is longer only if the initiation reaction requires more time to reach the steady state. Therefore, the water solubility of the monomer determines the duration of interval I, which is faster for more water soluble monomers such as vinly acetates [4].

In the course of interval II, the particle numbers and the polymerization rate are considered as constant and the propagation reaction is proceeded by the addition of monomers which are provided by the monomer droplets [3]. The consumption of the monomer is ranging from ca. 10-20 to 60% monomer conversion during the particle growth stage [5].

Emulsion polymerization continues to take place in interval III when the complete consumption of the monomer droplets occurs. The polymerization rate starts to decrease because the disappearances of the monomer droplets lead to consumption of the monomers in the polymerization loci. However, there may be an abrupt increase in the polymerization rate because of the gel effect during Interval III. Gel effect occurs when a bimolecular termination reaction takes place between two very viscous polymeric radicals [5].

1.3.3 Quantitative aspect of emulsion polymerization

In order to define the overall rate of the polymerization and the molar mass development of the latex particles, initiation, propagation, termination and transfer reactions are applicable because emulsion polymerization is a kind of a free radical addition polymerization. However, heterogeneous characterization of polymerization makes kinetics more complicated due to the transfer of ingredients between phases namely: the micellar phase, the aqueous phase, the monomer droplet phase and particle phase. Polymerization reactions may take place in all phases at the beginning of the polymerization. However, when monomer droplets

start to disappear, polymerization shifts to the aqueous phase and then the particle phase in latter stages. It is said that polymerization taken place in particle phase is generally predominant in emulsion polymerization [3].

When a radical enters a micelle or a polymer particle, usually free radical polymerization takes place and the polymerization rate r_p is the product of the monomer concentration [M] and the polymerization rate constant k_p [4].

$$r_p = k_p[M] \tag{13}$$

The radical concentration in the particle nuclei is higher than those in the homogeneous polymerization systems and the life of the radicals lasts for only a few thousand of a second. The presence of the second radical in the particle nuclei leads to the bimolecular termination and in order to react with the particle nuclei another free radical needs to enter the polymerization medium. It is well known that emulsion polymerization takes place in an isolated compartment called particle nuclei, which prevents the propagation reaction from the other propagating radicals, which causes the molar mass of the polymer to be higher than that for solution polymerization [4].

The rate of the polymerization at any time depends on the concentration of the active particle $[P\cdot]$ and the rate of the propagation in a particle.

$$Rp = k_p[M][P\cdot] \tag{14}$$

and $[P\cdot]$ can be expressed as:

$$[P\cdot] = \frac{N^{'}n}{N_a} \tag{15}$$

where $N^{'}$ is the concentration of micelles plus particles, n is the average number of radicals per micelle plus particle, and N_a is the Avogadro number. Replacing $[P\cdot]$ with this equation gives polymerization rate as;

$$R_p = \frac{N^{'} n k_p [M]}{N_a} \tag{16}$$

Both the rate of the polymerization and the molar mass of the polymer are dependent on the average number of radicals per particles, n, which is the function of the rate of radical generation, the number of polymer particles, the efficiency of the entry and exit of radicals into the particles and the termination reactions. The water solubility of the monomers influences these factors and the average number of the particles is not constant in the course of polymerization. Smith and Ewart determined the three limiting cases for n. Case I was defined where $n \ll 0.5$.When the solubility of the monomer is high; the rate of the radical exit rate is greater than the rate of radical entry rate. Case II occurs when $n = 0.5$, which implies that rate of radical exit from the particle nuclei is trivial, termination is instantaneous and thus particles have zero or one propagating chain any point in time. Case III is defined where $n \gg 0.5$ which occurs when the rate of termination within the particles is smaller than the rate of the radical entry rate and the particle volume is comparatively large [3].

Smit-Ewart theory proposed the following equation by considering only the polymerization taking in the particle nuclei:

$$N = k\left(\frac{\rho}{\mu}\right)^{0.4} \left(a_s S\right)^{0.6} \tag{17}$$

where μ is the rate of the particle growth volume , k is the proportionality constant, ρ is the rate of radical generation, a_s is the area occupied by a surfactant molecule and S is the total amount of surfactant in the micelles [3].

1.3.4 Other emulsion polymerization techniques

Inverse emulsion polymerization technique involves a system in which an aqueous solution of a hydrophilic monomer is polymerized in a non-aqueous continuous phase such as xylene or paraffin and both oil-soluble and water-soluble initiator can be used in order to initiate polymerization in water-in-oil type colloidal systems. Acrylamides and other water soluble monomers are commercially polymerized or copolymerized by using the inverse emulsion technique [4].

In mini emulsion polymerization, the monomer droplets are in the range of 50-1000nm. Micelles formation is not observed because the surfactant concentration always falls below the critical micelles concentration (CMC). Monomer droplets are stabilized by both a surfactant and a costabilizer such as hexadecane and cetyl alcohol. The produced particle size is similar to monomer droplet size, which depends on the amount of surfactant and costabilizer and the amount of energy used in the homogeneous process. Eit

her water soluble or an oil soluble initiator can be chosen for mini emulsion polymerization. Monomer droplet size determines the reaction characteristic of the polymerization for example if the monomer droplet size is larger than 500 nm, suspension polymerization is observed and less than 500nm particle size causes emulsion polymerization. High solid content latexes is produced by using the mini emulsion polymerization route [4].

A microemulsion polymerization system involves monomer droplets ranging between 10-100 nm in diameter and since the surfactant concentration is higher than the critical micelles concentration, micelles are formed. Preferred initiators are

usually water soluble, but there are many studies that show oil soluble initiators are also usable.

Although there are visible similarities between conventional emulsion and microemulsion, only two intervals are observed in microemulsion polymerization. Large amounts of surfactant makes interval I longer, that is, the nucleation process take more time in microemulsion polymerization as compared to conventional emulsion polymerization. Moreover, there is no constant rate of polymerization in Interval II and the rate increases in time reaches a maximum then decreases [4].

1.4 Membranes

1.4.1 Historical development of membranes

Systematic studies of membranes can be traced to an eighteenth century scientist. Abbe Nolet first utilized the word “osmosis” to describe permeation of water through a diaphragm in 1748. During the nineteenth and early in twentieth century’s, membranes were only used as laboratory tools to develop physical and chemical theories. For example, Van’t Hoff used the measurement of solution osmotic pressure made with membranes by Troube and Pfeffer to explain the behavior of ideal dilute solutions. This study led to the construction of Van’t Hoff’s equation. Moreover, the development of the kinetic theory of the gases was achieved by using the concept of a perfectly selective semi permeable membrane by Maxwell and others. Later in the nineteenth century, collodion (nitrocellulose) membranes were used because of its reproducibility. In 1907, Bechhold developed a technique which used a route to produce graded pore size nitrocellulose membranes, other scientists produced commercial collodion membranes by improving Bechhold’s method. Important changes in membrane technology began with development of Loeb-Sourirajan process for making detect free, high flux, anisotropic reverse osmosis membranes. This technique inspires other scientists to

build up new membrane formation processes to produce high performance membranes. Ultrafiltration, microfiltration, reverse osmosis and electrodialysis method were all established before 1980 and the use of gas separation membranes was started with hydrogen separation in 1980. The last development in 1980 was the establishment of the pervaporization technique for dehydration of alcohol [6].

1.4.2 Types of membranes and their area of usage

The structure of the membrane determines the whole filtration process and the performance of the membranes. Membranes are generally classified as symmetrical (isotropic) and asymmetrical (anisotropic). Symmetrical membranes are uniform in composition and structure and homogeneous through the cross section of membranes, however, asymmetrical or anisotropic membranes have a layered structure with holes or pores of finite dimensions and they are chemically and physically heterogeneous. While thin and dense layers give selectivity for membranes, thick porous polymer layer provides support for the first layer [7].

Ceramic membranes are an asymmetric structure type of membrane with either dense or porous skin layer. Sintered ceramic particles (alumina (Al_2O_3), titania (TiO_2) and Zirconia (ZrO_2)) are used to produce rough porous support in reduced pore size before the formation of top layer occurs. The pore size necessary to support the final layer are range from 1 to 5µm. Ceramic membranes have some advantages. It is well known that absorption of water by a membrane meterails (swelling) increases the pore size, which causes a decrease in retention time and change in selectivity. Since swelling is not a problem for a ceramic membrane, an increase in pore size is not observed. Moreover, filtration of oils like fluid with high viscosity is achieved easily by ceramics membranes at very high temperature because ceramics are thermally stable. Since ceramic materials are chemically inert, they allow filtration of chemicals without any problems [8].

Hydrogen separation from gas mixtures are achieved by dense metal membranes with an asymmetrical structure such as especially palladium membranes, which have moderate stability against oxidation. Moreover, palladium membranes have high permeability and selectivity for hydrogen. Since the permeation rate through the membrane are inversely proportional to the thickness of the membranes and increase with increasing temperature, dense and tin membranes are mainly preferred [9].

Supported liquid membranes are a type of asymmetrical membranes, which are mainly used for the recovery of metal ions from an aqueous solution, the removal of contaminants from industrial effluents and the recovery of fermentation products [10]. High selectivity, simultaneous extraction and striping of desired elements by a proper carrier make supported liquid membranes attractive both in industry and in laboratory experiments [11].

Nanofiltration and reverse osmosis membrane can be prepared from nanocomposite material. A nanocomposite membrane is composed of a thin highly selective composite layer with porous supports which give mechanical strength. The thin selective layer determines the whole process and affects membrane performance. Polyamide, polyester amide, polyethylene and polysilane are good polymeric materials used for the production of thin film composite membrane. Moreover, polysulfones are utilized for the preparation of ultrafiltration and microfiltration substrate with good thermal and chemical stabilities [12].

Microporous membranes are a class of symmetric structure type of membrane having rigid highly voided structure with randomly distributed interconnected pores. The separation through the membrane depends on the size of pores. If material is to be completely separated from the other materials in a mixture, its size needs to be much smaller than the smallest pore of the membrane. When size of the material is between smallest and largest sized pores, it is partially rejected and if its size is greater than largest pore, it is completely rejected. Microporous membranes

are used in ultrafiltration and microfiltration processes for recovering valuable products as well as treating effluents and minimizing environmental problems [6].

In nonporous or dense membranes the molecules being transported across the membrane dissolve in the dense membrane matrix and then diffuse through it. Transport is achieved by diffusion under the driving force of a pressure, concentration or electrical potential gradient. A non porous dense membrane can be used to separate two identical particles in size if their solubility in membrane matrix is different. The dense membranes are mainly used in gas separation, pervaporation and reverse osmosis and in order to improve the flux, membranes with an anisotropic structure are preferred [6].

Electrically charged membranes can be dense or microporous and usually referred as ion exchange membranes. Ions carrying the same charge as the membrane material are more or less excluded from the membrane phase and, therefore, unable to penetrate through the membrane. In other words, a positively charged membrane binds the anions in the surrounding medium and allows the passage of anion through the membrane with a driving force. Electrolyte solutions in electrodialysis are processed by using electrically charged membranes [6].

1.4.3 Phase Inversion: Polymeric Membrane Preparation Process

Most of the commercially available membranes are produced with the phase inversion process because easy controlling and adjustment over the initial stage characterize the whole morphology and a membrane with porous or nonporous structure can be prepared with this method. Basically, controlled transformation of a polymeric solution from the liquid state into the solid state is called phase inversion. Membrane preparation starts with the transformation of a liquid phase into the two liquid state, which is referred to liquid-liquid demexing, then the liquid state with a higher polymer concentration is solidified and forms a membrane structure by the following methods solvent evaporation, precipitation with controlled evaporation, thermal precipitation, precipitation from the water phase and immersion

precipitation. In solvent evaporation, the polymer solution is poured on a porous or nonporous support then the solvent is allowed to evaporate in an inner nitrogen medium. A dense homogeneous membrane is produced as a result of the complete evaporation of the solvent. A porous membrane is also prepared by precipitation from the vapor phase technique. A cast film of polymer is placed in a vapor phase of a mixture of a nonsolvent saturated with solvent and diffusion of nonsolvent molecules into the cast film causes the formation of membrane structure. Precipitation by controlled evaporation is another technique in which polymer dissolves in a mixture of a more volatile solvent and its nonsolvent. Evaporation of solvent makes the polymer precipitate in nonsolvent and the process finishes by formation of a skinned polymer membrane structure. Moreover, there is thermal precipitation method that is generally used for preparing microfiltration membranes. In this method, the phase separation of solvent and the polymer occurs by cooling, followed by evaporation of the solvent leads to the formation of membrane. The last technique is referred to immersion precipitation. Commercially available polymer membranes are mostly produced by this method. In this process, polymer solution is poured on a support layer then dipped into a nonsolvent medium. Phase separation and exchange of the solvent and nonsolvent activate the polymer precipitation and membrane structure is formed immediately [13].

1.5 Membrane Separation Process

We can define a membrane as a selective barrier between two phases in which the passage of solutes or solvents through thin, porous membranes is achieved by active or passive transport of matters (Figure 1.3). Dead-end filtration and cross-flow filtration are the pressure driven membrane separation processes with liquid permeation. An operating system is called dead-end when retentate is not continuous. A system is called cross flow if there is continuous retentate stream from the module outlet [14]. In dead end filtration operation, the suspended solid in liquid medium that sits in the flow channel is pressed with a driven force of

pressure, so that all of the water passes through the membrane and most of the suspended solid in the liquid medium are left behind or trapped in the membrane (Figure 1.4). In cross flow filtration method, solid molecules suspended in liquid medium are to be forwarded parallel to membrane. While some of the suspended solid is filtered from the liquid, the remainder solids join the feed and start to reflow parallel to the membrane [15].

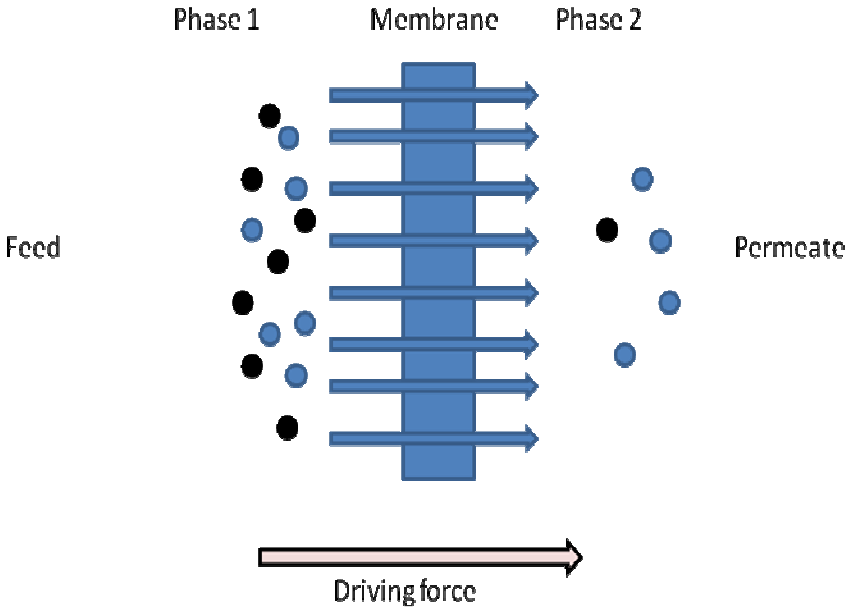

Figure 1.6 Schematic representation of a membrane

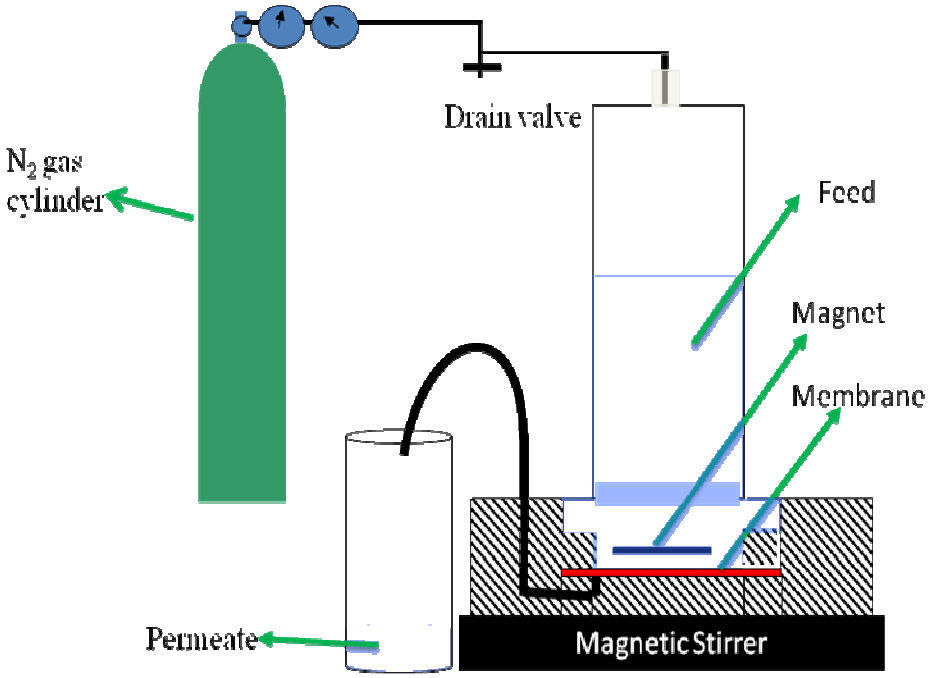

Figure 1.7 Schematic representation of dead-end filtration apparatus used in our experiments

The two parameter selectivity and the flow through membrane, also called permeation rate or flux, determine the performance of efficiency of a given membrane. The flux can be defined as the volume following through the membrane per unit area and time (unit of L/m^{2}h).

$$J = \frac{V}{At} \tag{18}$$

where V is the volume of solvent (water) (L), A is the active membrane area (m^2) and t is time interval (h).

The retention (R) or the separation factor (α) is the parameter in which one shows the selectivity of a membrane towards a mixture. Retention is more useful a expression of the selectivity when the filtration process is applied for a dilute aqueous solution of a solute. Partial or complete retention of solute molecules takes

place when solvent molecules pass easily through the membrane medium with a driven force. Retention can be expressed by the following equation:

$$R = \left(\frac{C_f - C_p}{C_f} \right) = 1 - \frac{C_f}{C_p} \tag{19}$$

where C_f is the solute concentration in the feed and C_p is the solute concentration in the permeate [13].

Membrane transport processes such as microfiltration, ultrafiltration and reverse osmosis depends on pressure as a driven force. Separation by an ultrafiltration and a microfiltration process is achieved by the sieving of molecules through the pores of the membranes. Colloidal particles and bacteria with a size ranging between 0.1 to 10 µm can be separated from their medium by microfiltration membranes. The ultrafiltration process is useful for the separation of macromolecules, such as proteins, from solutions.

Reverse osmosis membranes show very different mechanism of separation. A typical reverse osmosis membrane has a pore size ranging 3Å to 5Å and transport through the membrane occurs in the following way solutes permeate the membrane by dissolving in the membrane material and by diffusion down a concentration gradient. The key factors which determine the separation of the molecules by reverse osmosis process is their solubility and their mobility difference in the membrane. There is a fourth type of separation method namely nanofiltration in which pressure is also used as a driving force. Nanofiltration membranes have pore size ranging from 5 Å to 10 Å in diameter and intermediate between ultrafiltration and reverse osmosis membranes. While nanofiltration membranes are useful for separating di- and trisaccharides sucrose and raffinose with molecular diameter ranging from 10 Å to 13 Å, monosaccharide fructose with a molecular diameter of about 5 Å-6 Å cannot be filtered by these membranes [6]. Figure 1.5 summarizes the filtration process schematically.

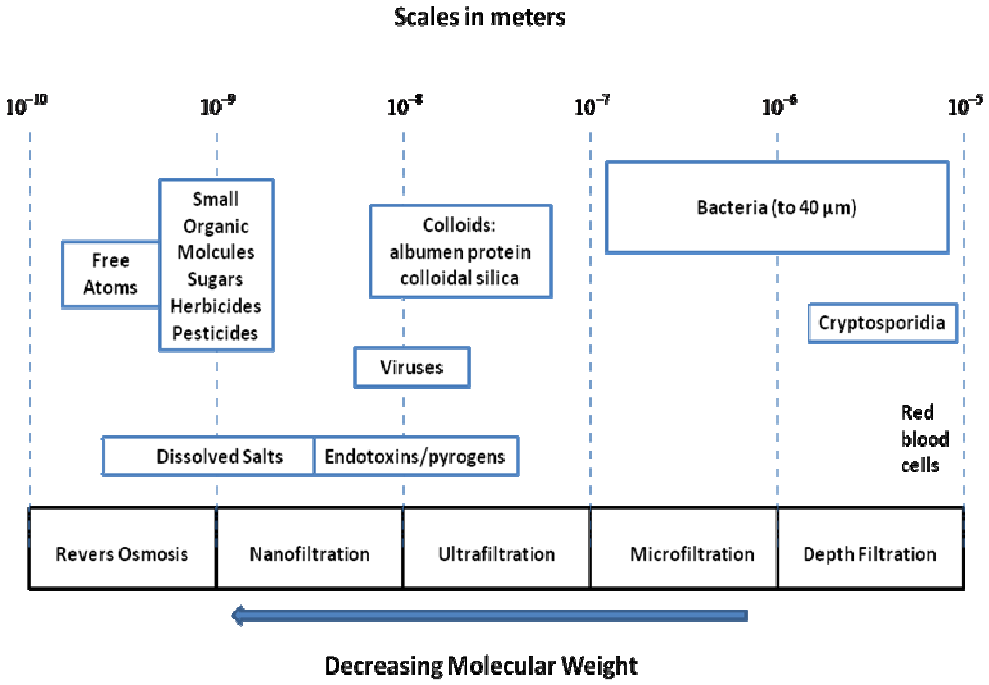

Figure 1.8 Relative Sizes of materials separated in membrane processes

1.5.1 Microfiltration

Separation of molecules by the microfiltration process depends on the pore size of the membrane, that is, a particle larger than the membrane pores are retained on the surface of the membrane and cannot pass through the pores. Microfiltration membranes fall between ultrafiltration membranes and conventional filters and are used to separates the colloidal particles and the bacteria from 0.1 to 10µm in diameters. It is well known that flux is proportional with the square of the pores. Therefore, microfiltration membranes have the highest flux per unit pressure difference (J/ΔP) among the reverse osmosis and the ultrafiltration membranes because a typical microfiltration membrane has a pore diameter of 10000 Å, which is 1000 times larger than ultrafiltration membrane pore and 100 times larger than the pore diamater of reverse osmosis. Therefore, the dramatic flux difference between the fluxes creates significant differences between the operating pressures

of the membranes process, which make microfiltration membranes industrially attractive [6].

1.5.2 Ultrafiltration

Ultrafiltration membranes have a porous type of membranes with more asymmetric structure as compared to microfiltration membranes. This asymmetric structure is composed of a thin and a supported layer. While the thin layer is responsible for mass transfer between the phases, the support layer gives mechanical strength to the membrane. Therefore, it is said that thin top layer determines the whole process of ultrafiltration. Since the typical pore diameter of ultrafiltration membranes are between the 20-1000 Å, which are much smaller than the pore size of microfiltration membranes, the pressure needed to operate filtration process is higher. Ultrafiltration membranes are mainly used in food and dairy, textile, chemical, pharmaceutical, metallurgy, paper and leather industries for separation of high molecular components from the low molecular components [13].

1.5.3 Nanofiltration

Nanofiltration membranes fall between ultrafiltration and reverse osmosis membranes and are used to separate salts with lower rejection but with much higher water permeability. While separation of sodium chloride with a reverse osmosis membrane is greater than 98%, this value falls to 20-80% when separation proceeds with a nanofiltration membrane. Moreover, organic solute molecules with molecular weight ranging from 200 to 1000 dalton can be separated with nanofiltration membranes. The separation process of salts is greatly dependent on the pore size of the membrane and the charge that attached itself to polymer backbones. Neutral nanofiltration membranes behave like a molecular sieve and a particle with a larger size than pore cannot enter the pores and are rejected. The

nanofiltration membrane is referred to anionic when if positively charged groups attach polymer backbones. While divalent cationic ions such as Ca^{2+} are repelled by these cationic backbones, divalent anions such as SO_4^{2-} pass through the nanofiltration membranes easily. This situation occurs in reverse when an anionic nanofiltration membrane is taken into consideration [6].

1.5.4 Reverse Osmosis

A semi permeable membrane is placed between a pure water solution and a salt solution, then, the diffusion of pure water through the membrane begins to dilute saline water. In order to compensate concentration on the sides, the transport of the pure water through the saline water take place and when equilibrium is achieved, water level of the salt solution side is above the freshwater side. This process is referred to as osmosis and the driving force responsible for the flow of water is called osmotic pressure. When pressure is applied opposite to the osmotic pressure the salt solution, the flow direction of the water can be reversed if the applied pressure is high enough and this process is referred to as reverse osmosis [16].

All colloidal or dissolved matter from an aqueous solution can be separated completely by using a reverse osmosis membrane and almost pure water is obtained. Reverse osmosis membranes are also suitable for the filtration of concentrate organic solution but their areas of usage are mainly desalination applications [17].

The semi permeable property of the reverse osmosis membranes determines the whole process. While water permeates through the membrane easily, dissolved substances cannot pass and remain in the medium. The pressure required to start reverse osmosis process should be high enough to overcome the osmotic pressure. During the sea water desalination process, applied pressure is ranges from 55-68 bars [17].

1.6 Basic Information about the Chromium (VI)

Heavy metals in the aqueous environment have attracted a lot of attention because of potential health hazards to public health and living organism. Among these, chromium is one of the most dangerous heavy metal [18]. Common usage of chromate and dichromate in industries includes metal plating, pigment manufacturing, leather tanning and stainless production and leads to the production of Chromium, which has two oxidation states namely hexavalent and trivalent. When health hazards and impact on environment is to be considered, hexavalent form of the chromium must be examined because of its carcinogenic and mutagenic effects [18-20].

Cr (VI) is found in different oxy-anion forms depending on the pH and the total concentration of the solution. Cr (VI) is unstable and shows high oxidizing behaviors in the presence of the electron donor in the acidic medium. $HCrO_4^-$ is the dominant form of the chromium at pH 1 and pH 6 and only CrO_4^{-2} ions exist above pH 7 [19]. According to the Turkish Standard Institution and the World Health Organization, the tolerance limit for Cr (VI) in tap water is 0.05 mg/L and discharge into an inland surface is 0.1mg/L [21-22]. Since Cr (VI) has well known effects on environment and living organism, it is necessary to remove Cr (VI) from wastewater.

Chemical precipitation [23], electrochemical precipitation [23-24], reduction [25], adsorption [26], solvent extraction [27], evaporation, reverse osmosis and biosorption [28-30], ion exchange resins [31] are suitable techniques for the removal of chromium. However, they also have some disadvantages such as incomplete metal removal, expensive equipment, regular monitoring system, reagent or energy requirements or producing toxic sludge or other disposal waste products [32]. On the other hand, membrane separations methods including microfiltration, ultrafiltration, nanofiltration and reverse osmosis can be adopted to remove the chromium from wastewater without any formation of sludge.

1.7 Literature Review

Nowadays, there is a high level of industrial interest for polymeric nanoparticles for many special applications, for instance, ion adsorbent, fillers in polymers, pigments, calibration standards, diagnostic, drug carrier, reaction catalyst, environmental protection etc. The wide ranges of the application area of these nanoparticles are due to their simple production by many different monomers by simple dispersion and by the emulsion polymerization process. Lior Boguslavsky, Sigal Baruch and Shlomo Margel prepared Polyacrylonitrile nanoparticles by dispersion and emulsion polymerization in a continuous aqueous phase in the presence of an initiator and surfactant and investigated the effects of various polymerization parameters on the nanoparticles. They found that reaction parameters, i.e, monomer concentration, initiator concentration, surfactant type and concentration, temperature and time, ionic strength, pH and co-solvent concentration, all affects the size and the size distribution, yield and stability, reaction pathway etc. and used the results in order to define the optimal condition for preparing PAN nanoparticles [33].

The strong mutual interaction between the chains and the crystalline nature make the polyacrylonitrile suitable material in the textile industry and in housing and packing applications. However, it is due to the strong interaction between chains that polyacrylonitrile is not soluble in its monomer, which makes homopolymerization of polyacrylonitrile by a conventional emulsion polymerization process difficult. Katarina Landfester and Marcus Antonietti reported that the microemulsion polymerization technique is more suitable for homopolymerization where the polymer is not soluble in its monomer. Polyacrylonitrile with a size ranging from 100 to 180nm were produced by microemulsion polymerization and this was proved by TEM, wide range X-RAY and dynamic light scattering [34].

Many studies reported that different monomers can be used for the copolymerization of acrylonitrile. The conductive copolymer of poly (aniline-co-acrylonitrile) was synthesized by inverted emulsion polymerization route using

benzoyl peroide (BPO) as a novel oxidizing agent. T. Jeevananda and his coworkers found that even if the polyacrylonitrile concentration in the copolymers increased up to 80%, the order of conductivy of the copolymers remains the same. They reported that this may be due to the participation of both the $-C \equiv N$ groups of polyacrylonitrile and the $-NH$ groups of PANI in doping process [35]. Copolymerization of butyl acrylate and acrylonitrile in concentrated emulsion was carried out and the effects of the various reaction conditions on polymerization rate were investigated in this research [36]. Another study showed that a polyacrylonitrile-co-polybutyl acrylate copolymer is suitable material in order to prepare the gel electrolyte for lithium ion batteries. Firstly, copolymer was produced with classical free radical emulsion polymerization, then, phase inversion process was used to prepare microporous membranes [37]. Moreover, Eli Ruckenstein and his coworkers successfully synthesized the copolymer of acrylonitrile and the vinyl acetate by the concentrated emulsion polymerization process and found that longer reaction time is required for high molecular weight polymer and high fraction of AN and high amounts of initiator also increase the molecular weight [38].

Nanofiltration, ultrafiltration, microfiltration and composite membranes can also be prepared from polyacrylonitrile copolymer. Polyacrylonitrile based membranes have good chemical stability and good performance in aqueous chemical applications. In this work, although citric acid, sodium hydroxide and sodium hypochlorite were filtrated by using PAN based membranes, the membranes did not lose their performance [39]. In another study, polyacrylonitrile based ultrafiltration membranes and polyacrylonitrile-acrylic acid composite membrane were prepared and used for the water treatment processes and composite membranes showed better performance. The effect of the composition on the casting solution, the annealing process and the hydrophilic processing of membrane surface on the performance of the membranes were also investigated [40]. Anil Kumar and Sonny Sachdeva reported that poly (styrene-co-acrylonitrile) based composite membranes have the ability to separate chromic acid from aqueous medium. They also investigated

various experimental variables such as pressure, pH etc. on the membrane performance [41]. Polyacrylonitrile is a proper material for preparation of nanofiltration membranes. According to this research paper, nanofiltration membranes can be prepared from the PAN ultrafiltration membranes. While Lewis acid treatment following by sodium hydroxide treatment increases the density of the functional groups (in addition to –CN, -COONa and $–CONH_2$) on the pore surface, application of drying process for ultrafiltration membranes decreases the number of pores. As a result of this preparation process, nanofiltration membranes were prepared [42].

While poly (2-ethylhexyl acrylate) are produced by conventional emulsion polymerization route in an uncontrolled manner, recent miniemulsion polymerization technique provides more control over the polydispersity and molecular weight and it is suitable for the production of this polymer. P2EHA finds for itself several area of usage such as pressure sensitive adhesives because of its low Tg -50, good oil resistance and adhesion to various substrates [43]. A copolymer of poly (acrylic acid-co-2ethylhexy acrylate) was used to prepare films for mucoadhesive transbuccal drug delivery. To obtain the optimal mucoadhesion properties for poly acrylic acid, its polarity should be reduced and fluidity should be increased. Therefore, 2EHA monomers were used to prepare copolymer of PAA for this purpose. Results showed that incorporating 2EHA into the PAA polymer enhanced mucoadhasive performance of PAA [44]. Marc A. Dube and his coworkers synthesized the poly (2-ethylhexyl acrylate-co-vinyl acetate) copolymer by the miniemulsion polymerization technique by using a mixture of an anionic and a non-ionic surfactant. Later, the influence of the monomer, the chain transfer agent and the surfactant concentration on droplet size was investigated. Results showed that different combinations of surfactants affect the droplet size and the stabilization of droplets that polymerize [45].

In order to prepare Poly (n-alkyl (oxy)-n-hexyl acrylates) copolymer, oxoalkyl acrylates of long chain 7-oxo alcohols were synthesized as intermediate monomers

and monomers were characterized by IR, ^{1}HNMR and mass spectroscopy. Prepared copolymers from these monomers were also characterized. These copolymers are used as fluidity improvement for petroleum crude oils. Results showed that crude oils that were prepared from these copolymers have improved flow properties as compared to the crudes that were mixed with poly (n-alkyl acrylate) flow improvement [46]. Hexyl acrylate was polymerized by atom transfer radical polymerization techniques and its di- and tri block copolymer with methyl methacrylate were prepared. Polymerization was carried out by using different types of initiator and optimum polymerization conditions were determined in order to synthesis HA with well defined molecular weights and narrow polydispersity indices. Then, prepared homopolymer of hexyl acrylate were used in order to prepare di- and tri block copolymer and the characterization of all copolymers were done by GPC and ^{1}HNMR [47].

CHAPTER 2

EXPERIMENTAL

2.1 Acrylonitrile Copolymers Synthesis

2.1.1 Materials for Copolymer Synthesis and Nanoporous Filtration Membrane Preparation

Acrylonitrile (AN, 99%) and 2ethylhexyl acrylate (2EHA, 98%) (both supplied from Aldrich) were purified by vacuum distillation immediately before to use. A water soluble initiator, ammonium persulfate (APS, 99+ %), isopropyl alcohol (IPA) and sulfuric acid (all supplied from Acros Organics), which are technically pure, were used as received. 1-dodecanthiol (Merck) is preferred as a chain transfer agent. DOWFAX 8390 solution surfactant was used as received. Magnesium sulfate (97 % anhydrous), N, N- dimethyl formamide (DMF) (99.8%) and 1-methyl-2-pyrrolidonone (NMP) (99 %) were provided from Acros Organics and used as received. Deionized water was adopted as the polymerization medium. Emaraldine base polyaniline (supplied from Aldrich) was directly used while preparing nanoporous filtration membrane. 1, 5-Diphenyl carbazide from Merck were directly used for chromium detection.

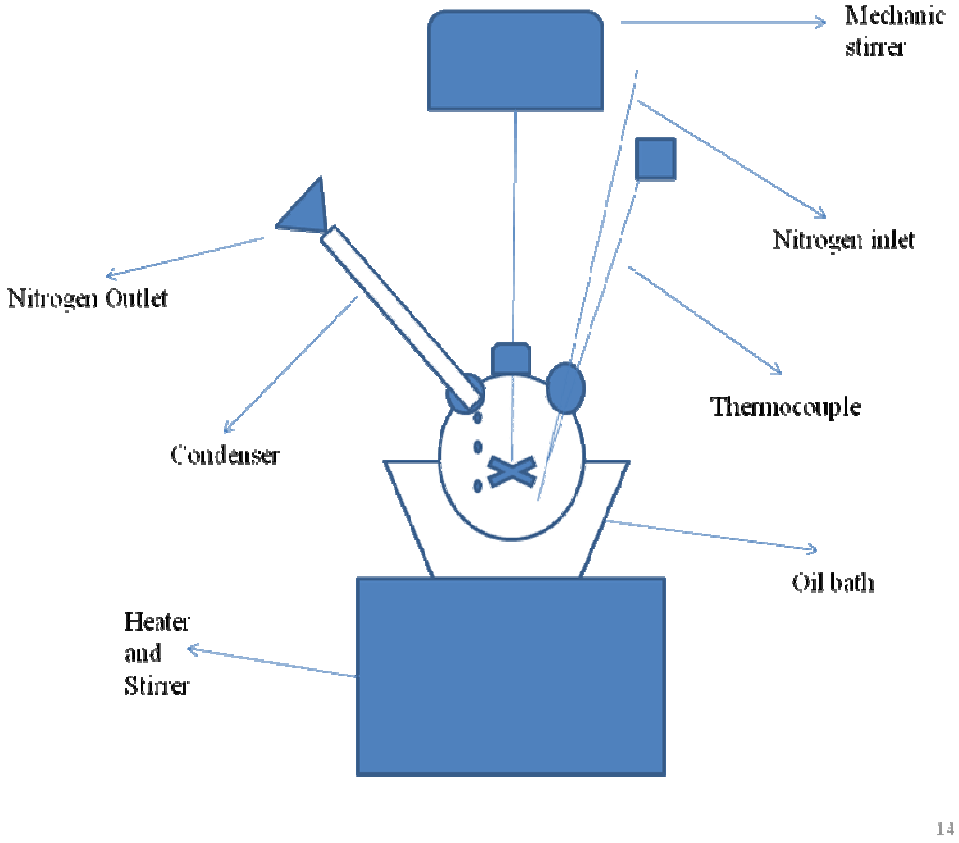

Figure 2.1 Schematic representations of experimental apparatus

2.1.2 Method for Preparation of Copolymers

The emulsion polymerization route was proceeded in order to synthesize the copolymer (Figure 2.1). Polymerization was carried out in an aqueous medium in the following order;

The following ingredients were mixed in a 250 mL three naked flask, which was fitted with a condenser, glass stirrer, dropping funnel, nitrogen inlet tube and a thermocouple probe was charged with water; water, surfactant, initiator (65% of total initiator), mercaptan and monomer mixture (20 % of total monomer). Before mixing ingredients, the temperature was raised to 68 $^{\circ}$C and the flask was purged with nitrogen for an hour. The remaining monomer mixture was added over a

period of 2h 30 min. After the addition of the monomer mixture, the remaining initiator was poured through the dropping funnel. The latex was held at 68 °C for an additional 45 min. The product was precipitated with 10% aqueous $MgSO_4$ solution and the copolymer was washed in distilled water for several times and left in isopropyl alcohol for overnight. The isopropyl alcohol removed any excess monomer that could still be present in the copolymer and also removed the water so the copolymer could be dried much easily. Finally, the product was vacuum dried at 62 °C overnight. Poly (acrylonitrile-co-hexyl acrylate) (PAN-co-PHA) and Poly (acrylonitrile-co-2ethylhexyl acrylate) (PAN-co-P2EHA) with various monomer concentrations were prepared (Table 2.1) and their physical and chemical properties were also investigated.

2.1.3 Nanoporous Filtration Membrane Preparation

For a typical 15 percent PANI composite, emaraldine base PANI (0.18 gram) were dissolved in DMF (8.0 gram) and mixed overnight. Then, the required amount (1,1gram) of PAN-co-P2EHA copolymer (intrinsic viscosity of 1.4dL/g) was added to the mixture to provide 15 percent PANI in the mixture. Later, the polymer mixture was poured on a smooth glass plate at room temperature and the plates were dipped into the IPA solvent for an hour. Finally, copolymer nanoporous filtration membranes were soaked in water at room temperature for an hour and doped with 1 M sulfuric acid solution for two hours then resoaked in water overnight. Membranes were permeated in water at 689.5 kPa prior to the performance tests.

2.1.4 Preparation of Nanoporous filtration membrane and Copolymer Films for FTIR

Nanoporous membranes were obtained the as same as mentioned previously. Prepared nanoporous membranes were then dried overnight and pounded in order to

obtain very small pieces and used in IR. The copolymer films were prepared by casting from DMF (6% wt/wt) on a smooth glass plate under a IR lamb at about 60 $^{\circ}$C and films were vacuum dried at 60 $^{\circ}$C for 2 hours for further drying.

2.2 Preparation of Synthetic Wastewater

An aqueous solution of chromium (500 mgL^{-1}) was prepared by dissolving potassium dichromate in ultra pure distilled water (ELGA, purelab option-Q). The aqueous solution was diluted with distilled water to obtain the Cr (VI) synthetic wastewater of desired concentrations. The pH of the solutions was adjusted using concentrated and 0.01 M NaOH/HCl using pH meter (Model wtw, Inolab).

2.3 Polymer Characterization Methods

2.3.1 Fourier Transform Infrared Spectroscopy (FTIR)

Perkin Elmer Spectrum100 FTIR spectrophotometer was used in order to record the IR spectra of the copolymer and the nanoporous filtration membranes. Both prepared nanoporous filtration membranes and the copolymer films were used in recording FTIR spectrum. FTIR spectra were taken directly. The PAN-based copolymer films and nanoporous filtration membranes were analyzed at 400-4000 cm^{-1}.

2.3.2 Nuclear Magnetic Resonance Spectroscopy (NMR)

^{1}H-NMR spectra of polymers were obtained by Bruker 300 MHz NMR spectrometer (BioSpin, Ettlingen, Germany). DMSO-d6 was used as a solvent. The sample concentration was approximately 8 mg/ml. The proton signals were

referenced to tetramethylsilane (TMS) at 0 ppm as the internal standard. The data were evaluated by using XWINNMR software.

2.3.3 Differential Scanning Calorimetry (DSC)

The glass transition temperature (T_g) of the copolymers were evaluated by Perkin Elmer Diamond DSC under nitrogen atmosphere with a heating rate of 10 $^{\circ}$C/min.

2.3.4 Thermogravimetric Analysis (TGA)

Thermal stability and thermal decomposition investigations of PAN-based copolymers and homopolymers were achieved by thermogravimetric analysis using a Perkin Elmer Pyris 1 TGA instrument (USA) under N_2 atmosphere with a heating rate of 10 $^{\circ}$C/min.

Table 2.1 Recipe for Emulsion polymerization of acrylonitrile based copolymers

Acronym	AN(g)	2EHA(g)	HA(g)	Initiator(g)	Surfactant(g)	C.T Agent(g)	Water(ml)
PAN(84)-co-PHA(16)	22.7	-	12.7	0.035	2.83	0.67	47
PAN(88)-co-PHA(12)	22.6	-	9.09	0.031	2.54	0.60	47
PAN(92)-co-PHA(8)	22.6	-	5.79	0.028	2.27	0.54	47
PAN(84)-co-P2EHA(16)	22.6	15.0	-	0.038	3.03	0.72	47
PAN(88)-co-P2EHA(12)	22.8	10.7	-	0.033	2.66	0.63	47
PAN(92)-co-P2EHA(18)	22.5	6.8	-	0.029	2.35	0.56	47

*The numbers in parentheses indicating the mole fraction of comonomer in polymers.

*PAN-co-PHA and PAN-co-P2EHA are acronyms used for Poly (acrylonitrile-hexyl acrylate) and Poly (acrylonitre-2ethlyhexyl acrylate) respectively.

2.3.5 Intrinsic Viscosity measurement

A copolymer was allowed to dissolve in -methyl-2-pyrrolidonone (NMP) and the intrinsic viscosity (IV) measurements were then performed by an Ubbelohde viscometer at 30°C. For each polymer, the viscosity of four concentartions was measured. Multiple readings were made at each concentration. Intrinsic viscosity was obtained by extrapolation of a plot of specific viscosity/concentration vs concentration to infinite solution.

2.3.6 Scanning Electron Microscopy (SEM)

Morphology of copolymer and nanocomposite membranes (cross sections) were obtained with a Field emission scanning electron microscopy QUANTA 400F. The membranes were cryogenically fractured in liquid nitrogen and then coated with gold/platinium.

2.3.7 Sheet Resistivity Measurement

Sheet resistivity of the nanoporous filtration membranes were measured using a Lucas type Four Point Probe equipped with Keithley 2400 IV Source Measure Unit. Errors resulting from film anisotropy were minimized by measuring the conductivity at different spots on the film. The average of these measurements has been reported in this study.

2.3.8 Swelling Ratio Measurements of Copolymer of PAN (92)-co-P2EHA (8) and PAN (92)–co-P2EHA (8)–PANI Nanoporous Filtration membranes

Swelling ratio measurements were performed with 4 samples and their averages were reported. Copolymer and nanoporous filtration membranes were dried overnight at room temperature and weighed. Then after left in ultrapure water for 24

hours, membranes were reweighed and reported. The following equation was used to calculate the equilibrium swelling ratio (SR) of films:

$$SR(wt\%) = \frac{W_w - W_d}{W_d} x100 \quad (1)$$

where W_w is the weight of the wet sample (soaked in water at room temperature for 24h) and W_d is the weight of the fully dried sample.

2.3.9 Water flux and Cr (VI) Removal Tests of Membranes

Both water and permeate fluxes of solutions containing 50, 100 and 250 ppm chromium (VI) were measured by using Sterlitech^{TM} HP 4750 type Dead end filtration apparatus at 689.5 kPa. Moreover, rejection of chromium (VI) was evaluated for these solutions at three different pH (2, 5 and 7). 1.5-Diphneyl carbazide method [48] which was proposed by the American Public Health Association was used to analyze aqueous solutions of chromium (Perkin Elmer Lambda 35 UV-Vis Spectrophotometer). The membrane size used in this study was 50 mm in diameter and the membrane area was 8, 1 cm^2. Water and permeate flux were calculated using following equation (Equation 2) as a unit of L/m^2h for 20 mL permeates volume by measuring the time interval.

$$J = \frac{V}{At} \quad (2)$$

where V is the volume of water or chromate solution (L), A is the active membrane area (m^2) and t is time interval (h).

The chromium rejection, R, was calculated according to Equation 3;

$$R = 100x\left(1 - \frac{C_p}{C_F}\right) \quad (3)$$

C_P and C_F are the chromium concentration in the permeate and in the feed respectively.

Fouling anaylsis were conducted with continuous permutation at 689.5 kPa. After 4 hour filtration, membranes were washed for 1h at 25 ^{O}C with deionize water. Then, pure water flux of the washed membrane (Jw_1) was measured to evaluate the fouling capacities of the nanoporous filtration membranes.

Percent flux recovery (PFR) was calculated using following equation (Eq. (4))

$$PFR = 100x\left(\frac{Jw_1}{Jw}\right) \tag{4}$$

Fouling analyses were also done by calculating total flux loss (TFL) (Eq. (5)) which is sum of reversible and irreversible flux losses;

$$TFL = \left(1 - \frac{Jp}{Jw}\right) \tag{5}$$

Reversible flux loss (RFL) can be seen in Eq. (6)

$$RFL = \left(\frac{Jw_1}{Jw}\right) - \left(\frac{Jp}{Jw}\right) \tag{6}$$

also, irreversible flux loss (IRFL) is defined by Eq. (7)

$$IRFL = \left(1 - \frac{Jw_1}{Jw}\right) \tag{7}$$

CHAPTER 3

RESULTS AND DISCUSSION

3.1 Poly (acrylonitrile-co-hexyl acrylate) Copolymers

Poly (acrylonitrile-co-hexyl acrylate) copolymers (PAN-co-PHA) at three different comonomer compositions (8, 12, 16 molar percent of poly (hexyl acrylate) (PHA))) were synthesized by emulsion polymerization in aqueous medium. FTIR and proton NMR were used in order to clarify their chemical structures and compositions. Molecular weights of the copolymers were characterized by intrinsic viscosity. Thermal properties of copolymers were also investigated by DSC and TGA.

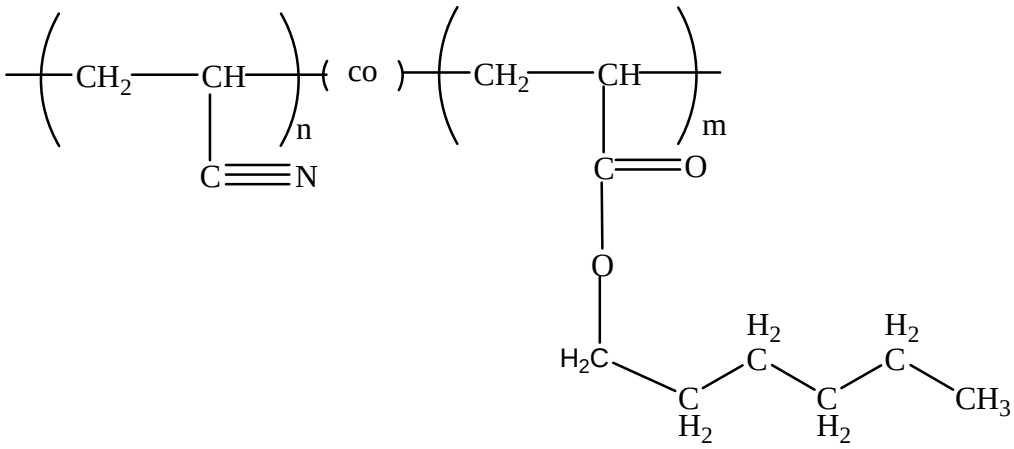

Figure 3.1 Chemical structure of poly (acrylonitrile-co-hexyl acrylate) (PAN-co-PHA) copolymer

3.1.1 Fourier Transform Infrared Spectroscopy (FTIR) Results

The FTIR spectra of the copolymers can be seen in Figure 3.2. The aliphatic CH_x asymmetric and symmetric stretching peaks were observed at 2923 and 2838 cm^{-1}, respectively. The characteristic -C≡N stretching peak was seen at 2229 cm^{-1} and -C=O stretching at 1728 cm^{-1}. The strong band at 1443 cm^{-1} corresponds to the CH_x bending. The peaks between 1351 1043 cm^{-1} were assigned to C-C-O and O-C-C ester stretching vibrations respectively. The chemical structures of the copolymers were confirmed by FTIR study.

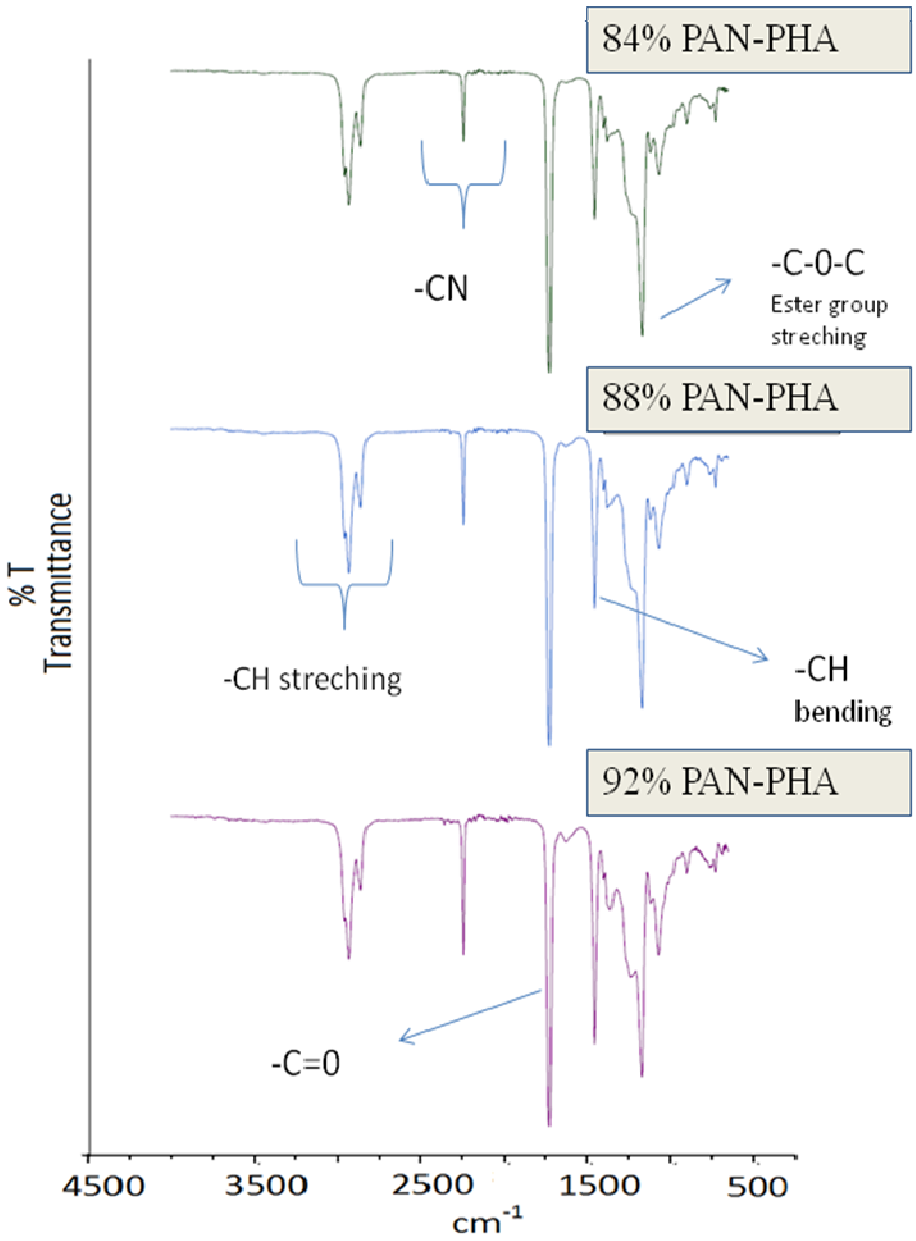

Figure 3.2 FTIR spectra of the copolymers; monomers were successfully incorporated to chemical structure.

3.1.2 Nuclear Magnetic Resonance Spectroscopy (NMR) Results

In order to confirm the chemical structure of the copolymer, ^{1}H-NMR spectrum (Figure 3.3) of PAN-co-PHA copolymers at various molar ratios was performed. The resonance between 3.18-2.80 ppm were assigned for –CH groups attaching –CN and carboxyl groups (c) and resonance at 4.12 ppm belonged to -OCH_2 stretching (b). The resonance peaks appeared between 2.2 ppm to 0.82 ppm were for hydrogen attaching –CH_2-CH_2-CH_2-CH_2-CH_3 (a) and the –CH_2 (a) backbone protons of hexyl acrylate and acrylonitrile. Moreover, copolymer composition was calculated by using the integral values of the following peaks and method:

-CH_2 backbone protons of acrylonitrile and hexyl acrylate and protons of –CH_2-CH_2-CH_2-CH_2-CH_3 of hexyl acrylate comonomer (a).

-OCH_2 (b)

The two protons from –OCH_2 give:

$$2m = x$$

$$m = \frac{x}{2}$$

The integral values of protons labeled as (a) give:

$$10m + 2n = y$$

$$n = \frac{y}{2} - 5m$$

$$n = \frac{(y - 5x)}{2}$$

Finally, percent composition of acrylonitrile incorporated into copolymer was calculated by the following equation:

$$\%AN = \frac{n}{(n=m)} x100$$

In order to obtain the percent of hexyl acrylate in the copolymer, the value of the percent acrylonitrile was subtracted from a value of 100%:

$$\%HA = 100 - \%AN$$

The actual compositions were calculated from ^{1}H-NMR (Table 3.1) and results can be seen in Table 3.2.

Table 3.1 Calculation of PAN composition in copolymer

92% PAN-co-PHA	88% PAN-co-PHA	84% PAN-co-PHA
2m=1 m=0.5	2m=1 m=0.5	2m=1 m=0.5
10m + 2n = 15.79	10m + 2n = 11.90	10m + 2n = 9.96
n=5.395	n=3.45	n=2.48
AN% = 100*n/(m+n)	AN% = 100*n/(m+n)	AN %= 100*n/(m+n)
100*(5.395)/(5.395+0.5)	100*(3.35)/(3.45+0.5)	100*(2.48)/(2.48+0.5)
AN%= 91.5%	AN= 87.3%	AN%= 83.2%

Table 3.2 Theoretical and experimental composition data of PAN-co-PHA copolymers

Sample(AN/HA)	Monomer feed (Molar ratio of AN to HA)	Composition (Molar ration of AN to HA)
92 % PAN-co-PHA	92/8	91.5/8.5
88 % PAN-co-PHA	88/12	87.3/12.7
84 % PAN-co-PHA	84/16	83.2/16.8

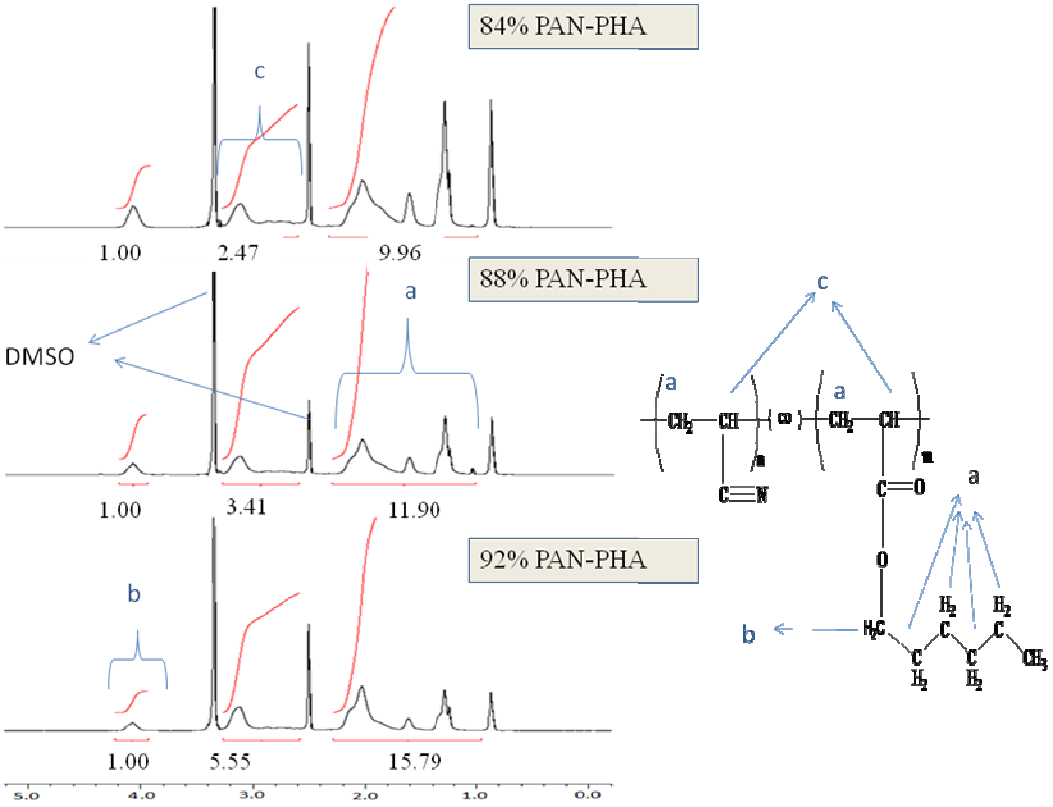

Figure 3.3 ^{1}H-NMR spectrum of PAN-co-PHA copolymers with different compositions; chemical structure was proved by ^{1}H-NMR

3.1.3 Intrinsic Viscosity Measurement

Intrinsic viscosities of copolymers were measured with a Ubbelohde viscometer at 30°C and results were given at table 3.3. Although the copolymers had sufficient molecular weight to form nanoporous filtration membranes, the dead end filtration measurement revealed that the nanoporous filtration membranes prepared from PAN-co-PHA copolymer were not suitable materials to remove Cr(VI) from water because both water fluxes and permeate fluxes were very low and chromium (VI) rejection was not achieved successfully.

Table 3.3 Intrinsic Viscosities of copolymers

Sample(AN/HA)	Monomer feed (Molar ratio of AN to HA)	$[\eta]_{30^\circ C}^{NMP}$ (dL/g)
PAN-co-PHA	92/8	1.4
PAN-co-PHA	88/12	1.1
PAN-co-PHA	84/16	1.3

3.1.4 Differential Scanning Calorimetry (DSC) Results

Copolymers of poly (acrylonitrile-co-hexyl acrylate) with various comonomer compositions were synthesized and their glass transition temperatures were determined from DSC. T_g data listed in Table 3.4 and showed that increase in mole fraction of hexyl acrylate comonomer caused a decrease in the glass transition temperature. T_g values of poly (acrylonitrile) and poly (hexyl acrylate) polymers are reported at 103 ^{O}C and -51 ^{O}C respectively [49, 50] and the obtained values of T_g of synthesized copolymer lies between these reported values.

Table 3.4 Glass Transition Temperature of Copolymers

Sample(AN/HA)	Monomer feed (Molar ratio of AN to HA)	T_g values of copolymer
PAN-co-PHA	92/8	69
PAN-co-PHA	88/12	56
PAN-co-PHA	84/16	52

3.1.5 Thermogravimetric Analysis (TGA) Results

Degradation temperature and weight loss behavior of copolymers were investigated by Thermalgravimetric analysis during successive heating over a period of time. Thermogram revealed that the percentage of the comonomer incorporated into the copolymer affected the thermal behavior. The TGA thermograms of the synthesized copolymers are shown in Figure 3.4. All of the copolymers are thermally stable up to 372 $^{\circ}$C which was high enough for many high temperature applications (Figure 3.5). Two step degradations were observed for copolymer which attributed to the side and the main chain degradation and this behavior can be clearly seen in Figure 3.4. 10% weight loss temperatures of copolymers are close to each other, which can be seen in Table 3.5.

Table 3.5 Thermal decomposition properties of copolymers (heating rate 10°C/min, N2 atmosphere)

Sample name	Composition (mol percent)	T_{10}[a] (°C)
Poly(acrylonitrile-co-hexyl acrylate)	92/8	361
Poly(acrylonitrile-co-hexyl acrylate)	88/12	361
Poly(acrylonitrile-co-hexyl acrylate)	84/16	368

[a] Temperature for 10% decomposition

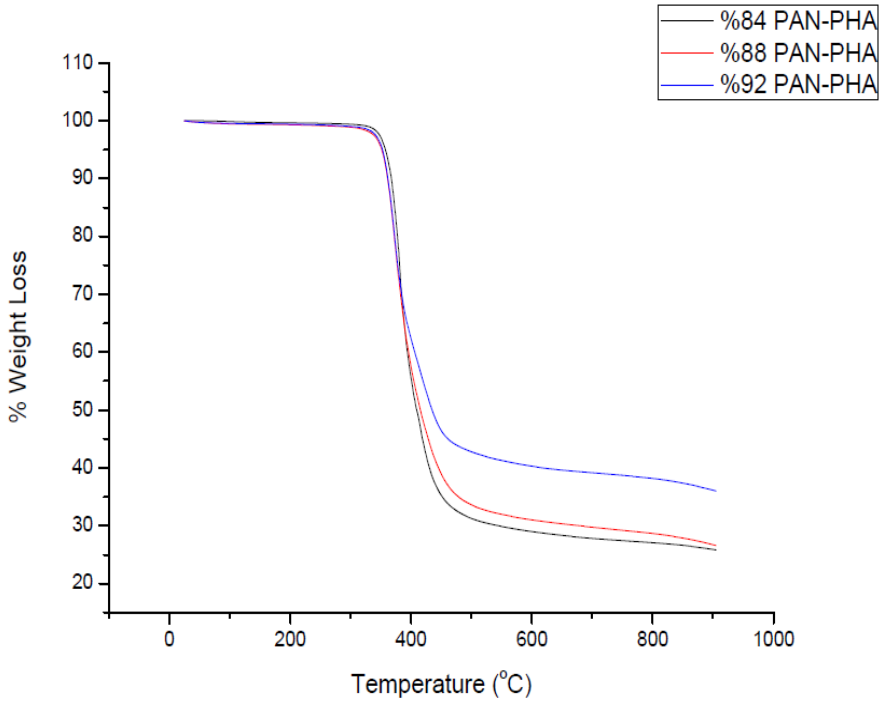

Figure 3.4 Weight loss temperatures for copolymers; copolymers were thermally stable.

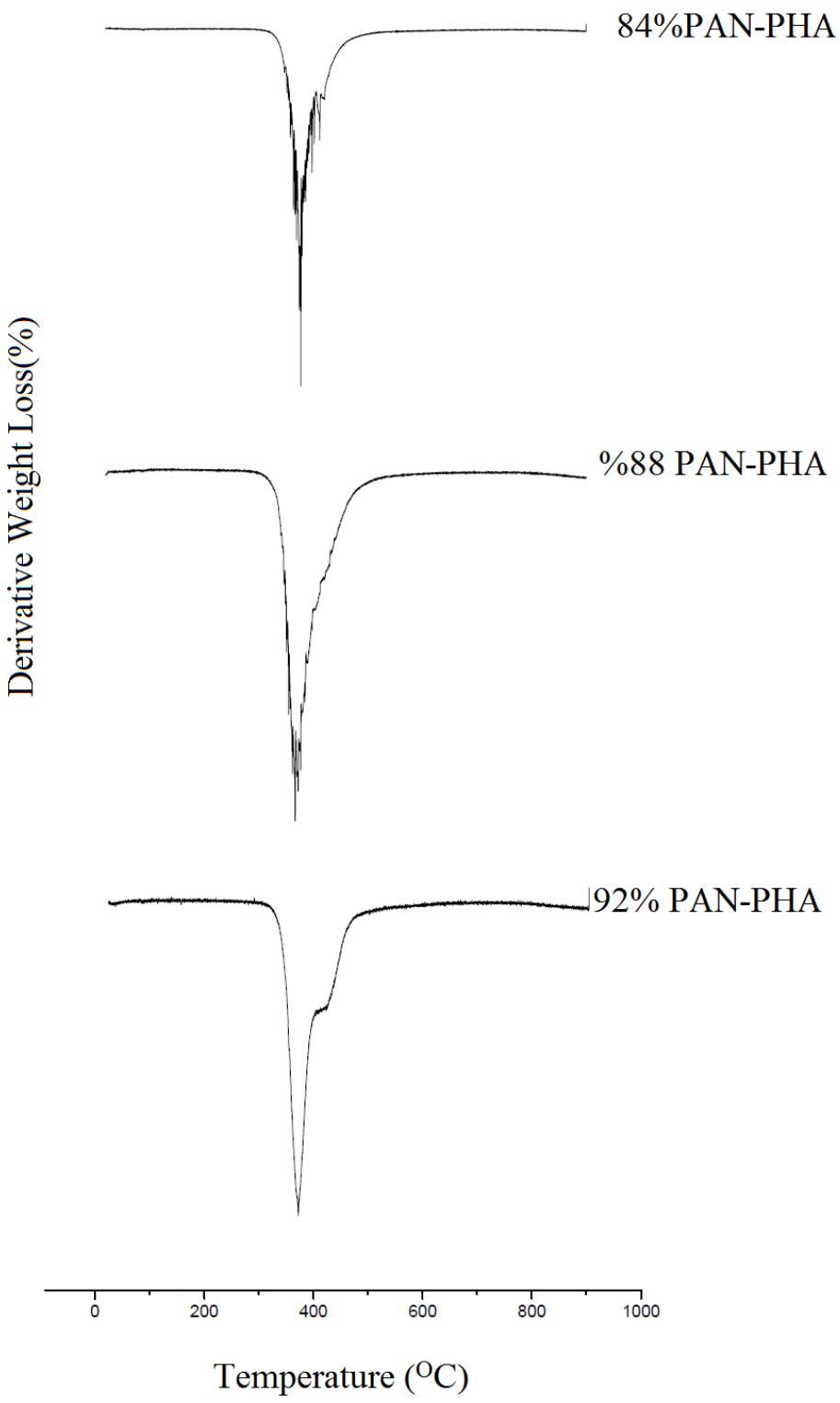

Figure 3.5 Derivative weight loss versus temperature curves of copolymer

3.2 Poly (acrylonitrile-co-2ethylhexyl acrylate) Copolymers

Poly (acrylonitrile-co-2ethylhexyl acrylate) copolymer (PAN-co-P2EHA) at three different compositions (8, 12 and 16 mole percent of poly2ethyl hexyl acrylate (P2EHA)) were synthesized by emulsion polymerization in an aqueous medium. Copolymers were characterized by FTIR, ^{1}H-NMR, NMR, intrinsic viscosity measurement, differential scanning calorimetry (DSC) and thermogravimetric analysis (TGA). Intrinsic viscosity measurements showed that molecular weight of the copolymers were sufficient to form nanoporous filtration membranes. The T_g values decreased with increasing the weight fraction of 2ethylhexyl acrylate. Moreover, the TGA results clarified that the stepwise thermal degradation was observed for copolymers and decomposition temperatures of copolymers were almost same.

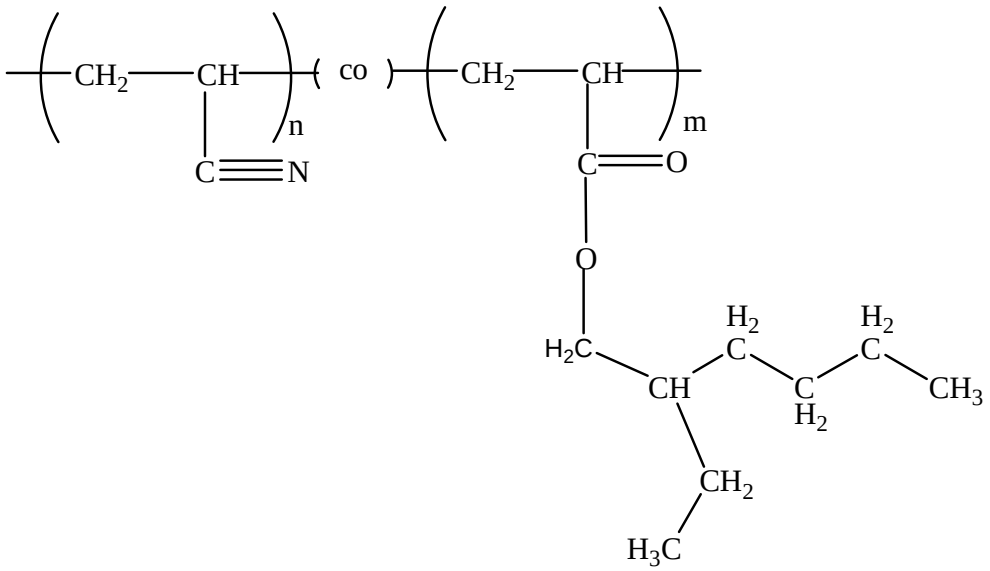

Figure 3.6 Chemical structure of poly (acrylonitrile-co-2ethylhexyl acrylate) (PAN-co-P2EHA) copolymer

3.2.1 Fourier Transform Infrared Spectroscopy (FTIR) Results

The FTIR spectrum of copolymer can be seen in Figure 3.2. The aliphatic CH_x asymmetric and symmetric stretching peaks were observed at 2929 and 2813 cm^{-1}, respectively. The characteristic -C≡N stretching peak was seen at 2278 cm^{-1} and -C=O stretching at 1713 cm^{-1}. The strong band at 1465 cm^{-1} corresponds to the CH_x bending. The peaks between 1281-1030 cm^{-1} were assigned to C-C-O and O-C-C ester stretching vibrations. The chemical structures of the copolymers were confirmed by FTIR study.

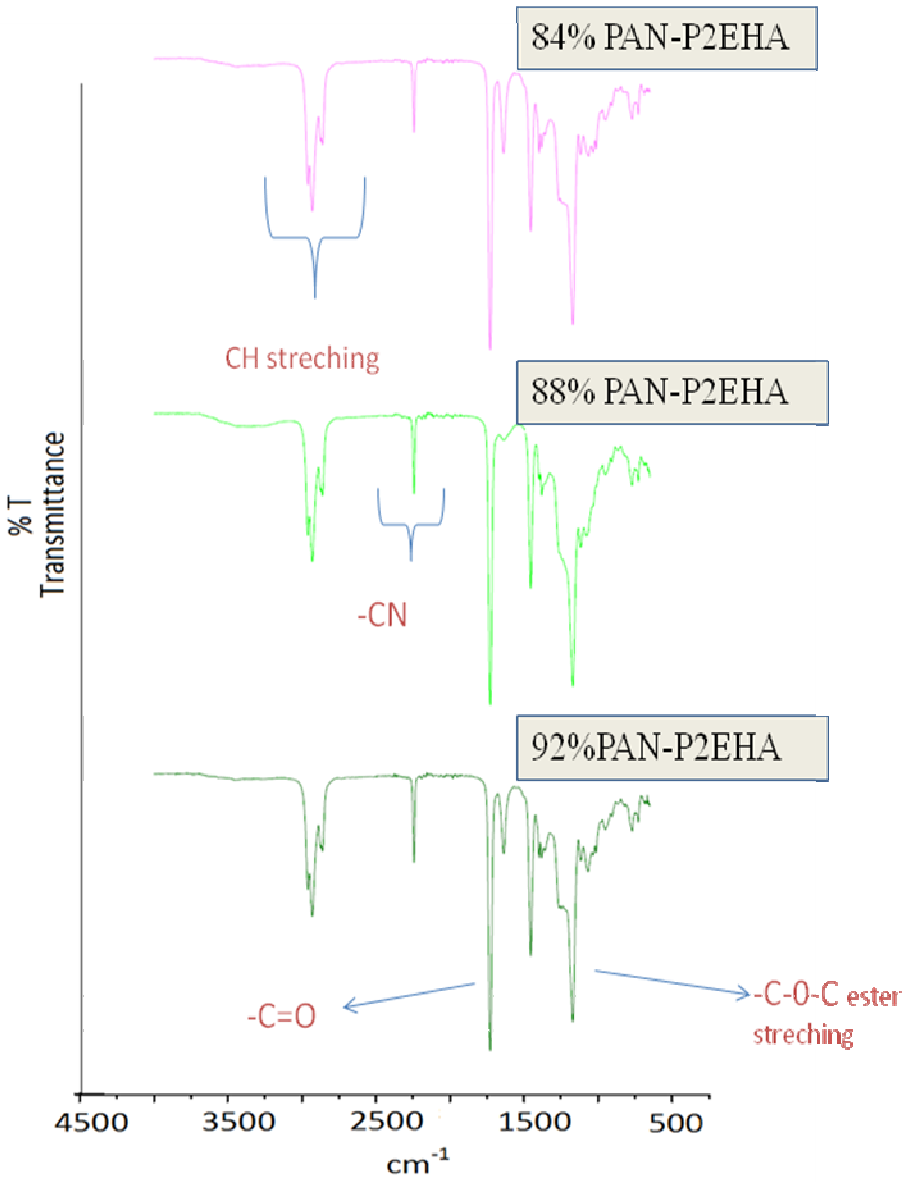

Figure 3.7 FTIR spectra of the copolymers; monomers were successfully incorporated to chemical structure.

3.2.2 Nuclear Magnetic Resonance Spectroscopy (NMR) Results

In order to confirm the chemical structure of copolymer, ^{1}H-NMR spectrum (Figure 3.8) of PAN-co-P2EHA copolymers at various molar ratios were performed. The resonance between 3.21-2.78 ppm were assigned for –CH groups attaching –CN

and carboxyl groups (c) and resonance at 4.08 ppm belonged to the -OCH_2 stretching (b). The resonance peaks appearing between 2.03 ppm to 0.8 ppm were for hydrogen attaching –CH_2-CH_2-(CH_2-CH_3)-CH_2-CH_2-CH_3 (a) and the –CH_2 (a) backbone protons of 2ethylhexyl acrylate and acrylonitrile. Copolymer composition was also calculated:

-CH_2 backbone protons of acrylonitrile and 2ethylhexyl acrylate and protons of CH_2-CH_2-(CH_2-CH_3)-CH_2-CH_2-CH_3 of 2ethylhexy lacrylate comonomer (a).

-OCH_2 (b)

The same calculation method was applied for the determination of the PAN-co-P2EHA copolymer composition and the calculation can be seen in Table 3.6 and the results in Table 3.7.

Table 3.6 Calculation of PAN composition in copolymer

92% PAN-co-P2EHA	88% PAN-co-P2EHA	84% PAN-co-P2EHA
2m=1 m=0.5	2m=1 m=0.5	2m=1 m=0.5
17m + 2n = 21.47	17m + 2n = 15.99	17m + 2n = 14.36
n=6.485	n=3.745	n=5.395
AN %= 100*n/(m+n)	AN %= 100*n/(m+n)	AN %= 100*n/(m+n)
100*(6.485)/(6.485+0.5)	100*(3.745)/(3.745+0.5)	100*(2.93)/(2.93+0.5)
AN%= 92.8 %	AN%= 88.2 %	AN%= 85.4 %

Table 3.7 Theoretical and experimental composition data of PAN-co-P2EHA copolymers

Sample (AN/2EHA	Monomer feed (Molar ratio of AN to 2EHA)	Composition (Molar ratio of AN to 2EHA)
92% PAN-co-P2EHA	92/8	92.8/7.2
88% PAN-co-P2EHA	88/12	88.2/11.8
84% PAN-co-P2EHA	84/16	85.4/14.6

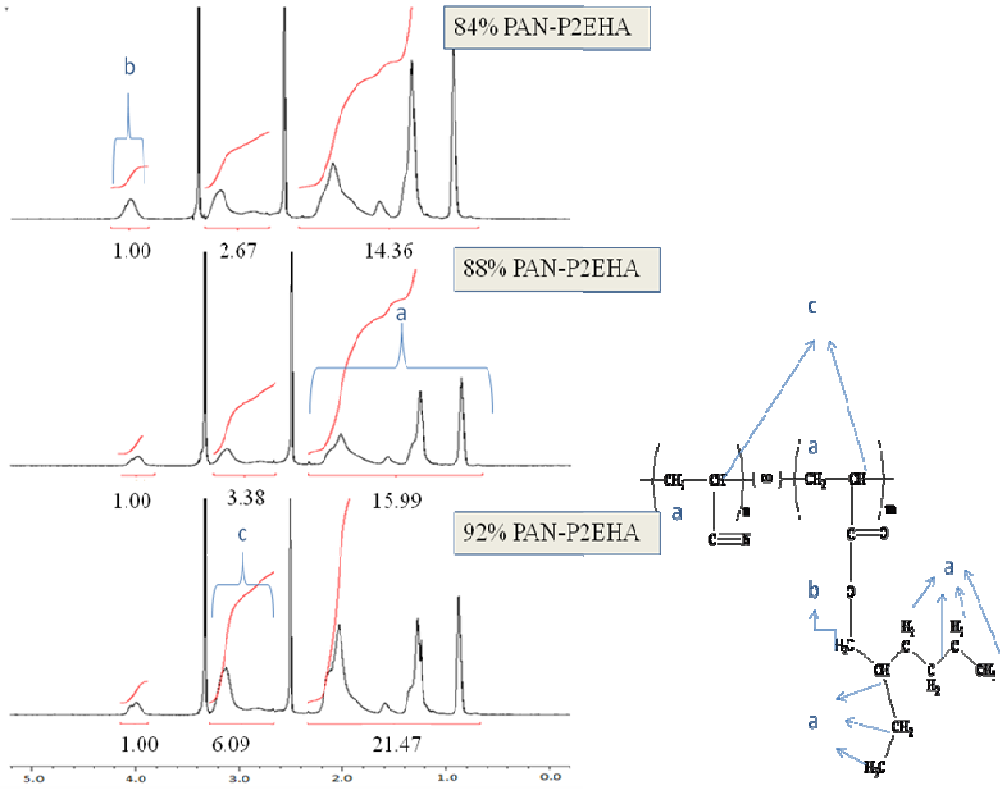

Figure 3.8 ^{1}H-NMR spectrum of PAN-co-P2EHA copolymers with different compositions; chemical structure was proved by ^{1}H-NMR

3.2.3 Intrinsic Viscosity Measurement

Intrinsic viscosities of the copolymers were measured with an Ubbelohde viscometer at 30°C and the results were given at table 3.3. %92 PAN-co-P2EHA copolymer had sufficient molecular weight to form nanoporous filtration membranes and dead end filtration measurement revealed that nanoporous filtration membranes prepared from %92 PAN-co-P2EHA copolymer were suitable materials to remove Cr (VI) from water. Chromium (VI) rejection was achieved successfully by using this copolymer.

Table 3.8 Intrinsic Viscosities of copolymers

Sample(AN/HA)	Monomer feed (Molar ratio of AN to HA)	$[\eta]_{30^oC}^{NMP}$ (dL/g)
PAN-co-P2EHA	92/8	1.4
PAN-co-P2EHA	88/12	1.0
PAN-co-P2EHA	84/16	0.8

3.2.4 Differential Scanning Calorimetry (DSC) Results

Copolymers of poly (acrylonitrile-co-2ethylhexyl acrylate) with various comonomer compositions were synthesized and their glass transition temperatures were determined from DSC. The T_g data listed in table 3.9 and showed that increase in the mole fraction of the 2ethlyhexyl acrylate comonomer caused a decrease in the glass transition temperature. T_g values of the poly (acrylonitrile) and the poly (2ethylhexyl acrylate) polymer are reported at -58 ^{O}C and 103 ^{O}C respectively [46, 49] and the obtained values of T_g of the synthesized copolymer lies between those reported values.

Table 3.9 Glass Transition Temperature of Copolymers

Sample(AN/HA)	Monomer feed (Molar ratio of AN to HA)	T_g values of copolymer
PAN-co-P2EHA	92/8	55
PAN-co-P2EHA	88/12	50
PAN-co-P2EHA	84/16	47

3.2.5 Thermogravimetric Analysis (TGA) Results

Thermal characteristics of poly (acrylonitrile-co-2ethylhexyl acrylate) copolymers were studied. Degradation temperature and weight loss behavior during successive heating over a period of time were investigated and the TGA thermograms revealed that the amount of the comonomer in the copolymer affected the thermal behaviors of copolymer. The TGA thermograms of the synthesized copolymers are shown in Figure 3.9. All of the copolymers are thermally stable up to 385 $^{\circ}$C which was high enough for many high temperature applications (Figure 3.10). Two step degradations were observed for copolymer which attributed to the side and the main chain degradation and this behavior can be clearly seen in Figure 3.9. 10% weight loss temperatures of copolymers are close to each, which can be seen in Table 3.10.

Table 3.10 Thermal decomposition properties copolymers (heating rate 10°C/min, N2 atmosphere)

Sample Name	Composition (mole percent)	T_{10}[a] (°C)
PAN-co-P2EHA	92/8	363
PAN-co-P2EHA	88/12	364
PAN-co-P2EHA	84/16	368

[a] Temperature for 10% decomposition

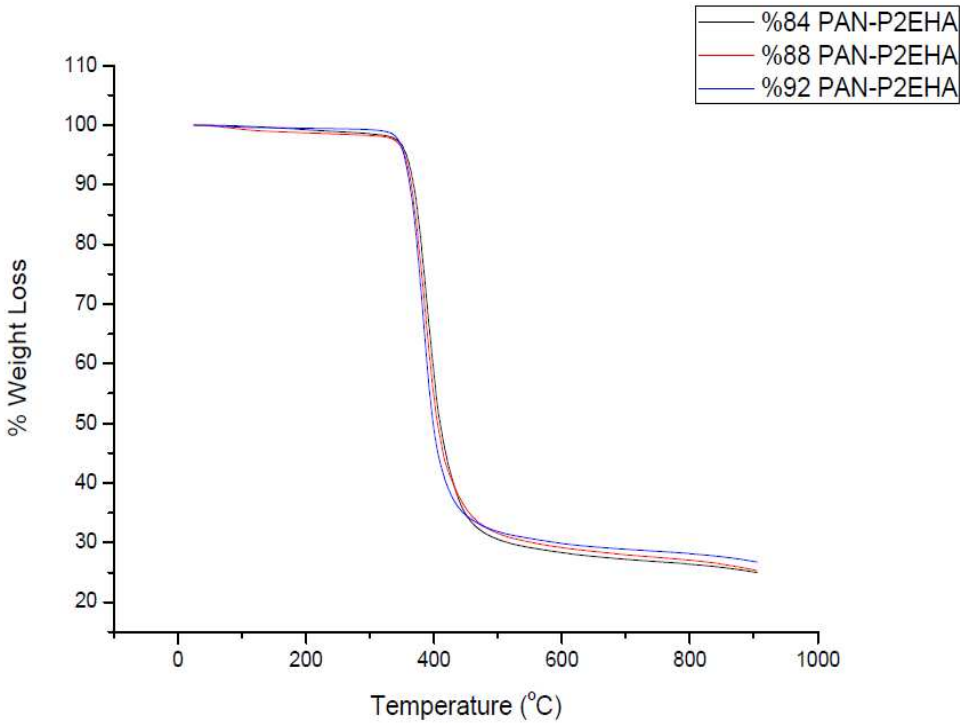

Figure 3.9 Weight loss temperatures for copolymers; copolymers were thermally stable.

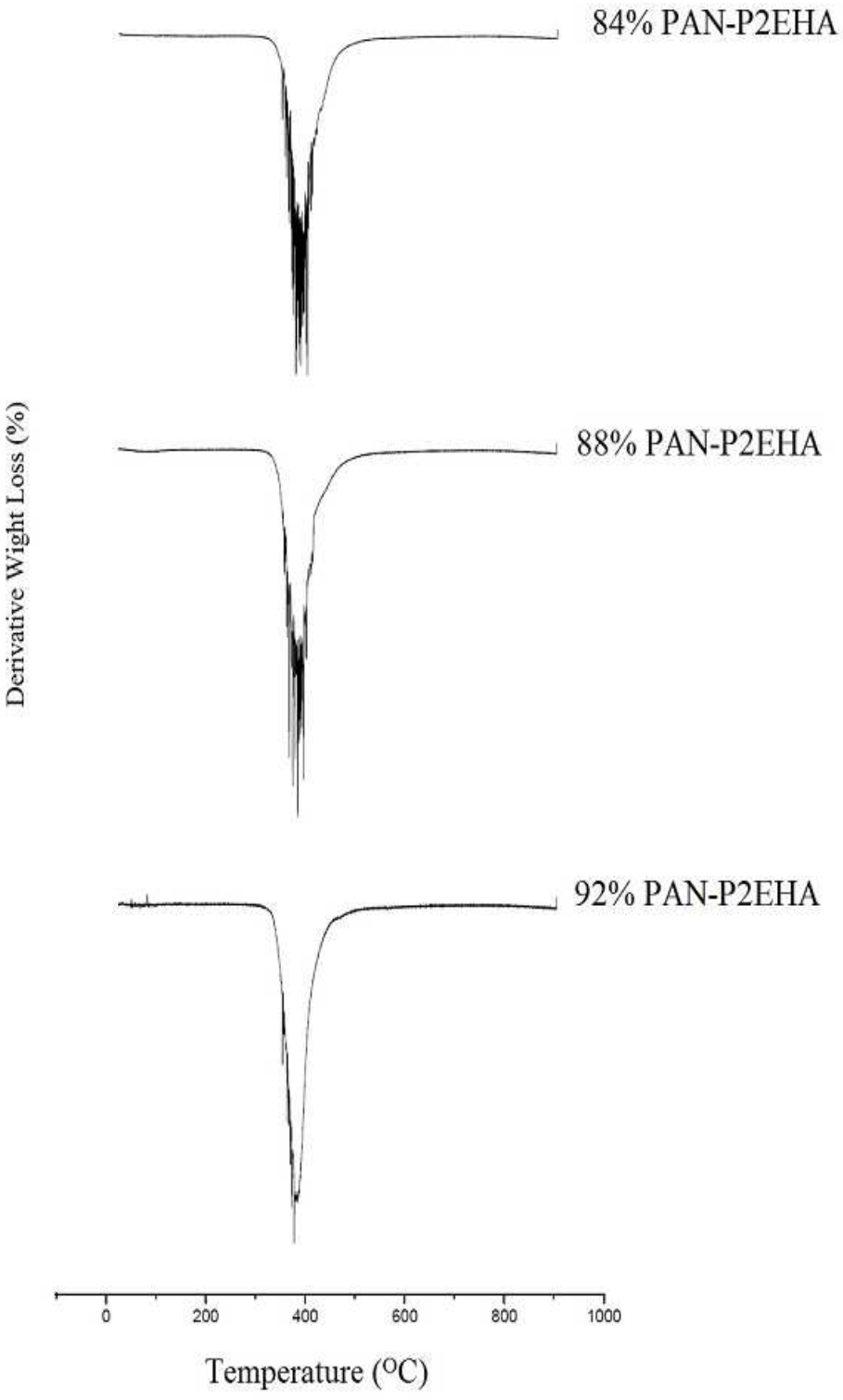

Figure 3.10 Derivative weight loss versus temperature curves of copolymer

3.3 Chromium (VI) Removal Performance of Nanoporous Filtration Membranes

Both poly (acrylonitrile-co- hexyl acrylate) and poly (acrylonitrile-co-2ethylhexyl acrylate) copolymer were converted into a nanoporous filtration membrane and their performance was tested with deadend filtration. Experimental results showed that the nanoporous filtration membrane prepared from poly (acrylonitrile-co-hexyl acrylate) copolymer had very low pure water fluxes so we further continued with the poly (acrylonitrile-co-2ethylhexyl acrylate) copolymer in order to remove the chromium (VI) from the water. Test results related to the poly (acrylonitrile-co-hexyl acrylate) nanoporous filtration membranes can be seen in Table 3.11.

Table 3.11 Pure water flux of nanoporous filtration membranes prepared from poly (acrylonitrile-co-hexyl acrylate) copolymers

Membrane	Pure water flux (L/m^2h)
PAN(92)-co-PAN8)-PANI(5)	98
PAN(92)-co-PAN(8)-PANI(10)	99
PAN(88)-co-PAN(12)-PANI(5)	94
PAN(88)-co-PAN(12)-PANI(10)	93
PAN(84)-co-PAN16)-PANI(5)	89
PAN(84)-co-PAN16)-PANI(10)	91

3.3.1 Chemical Structure of the Nanoporous Filtration Membranes Prepared from Poly (acrylonitrile-co-2ethylhexyl acrylate) with PANI

Electrically conductive polyaniline (PANI) polymer was used in order to prepare poly (acrylonitrile (92)-co-2ethylhexyl acrylate (8)) - PANI nanoporous filtration membrane solutions with three different PANI loadings by phase inversion. Prepared nanoporous filtration membrane solutions were then converted to nanoporous filtration membranes. Acid treatment was applied to nanoporous filtration membranes in order to turn emeraldine base to electrically conductive emeraldine salt.

The chemical structure of emeraldine based polyaniline was shown in Figure 3.11. Nanoporous filtration copolymer membranes were analyzed by FTIR analysis (Figure 3.12). Aliphatic CH and CN stretching of PAN (92)-co-P2EHA (8) copolymer were observed at 2923 cm^{-1} and 2329 cm^{-1} respectively. The ester group of methyl acrylate was detected typically at 1728 cm^{-1}. Characteristic peaks of benzoid and quinoid rings of polyaniline were observed at 1597 cm^{-1} and 1643 cm^{-1}. The peak at 1322 cm^{-1} was assigned to the angular deformation of CN group of polyaniline.

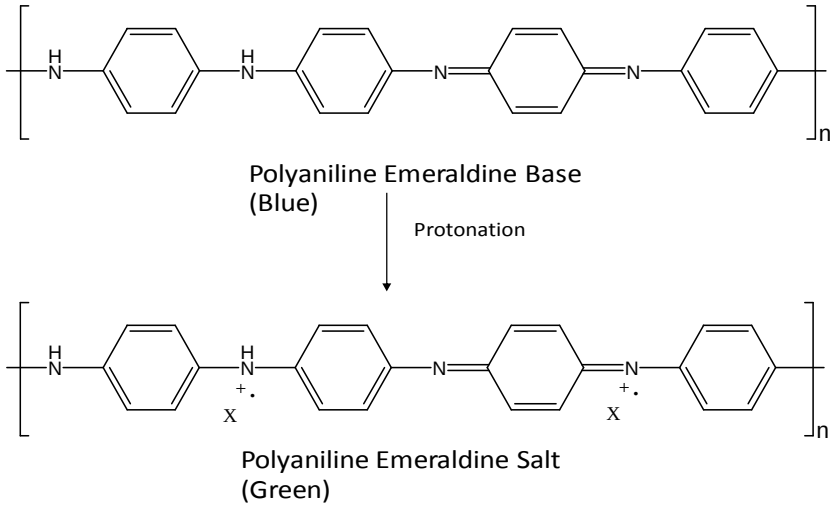

Figure 3.11 Chemical Structures of Emeraldine base and salt of PANI (X is dopant cation, H+)

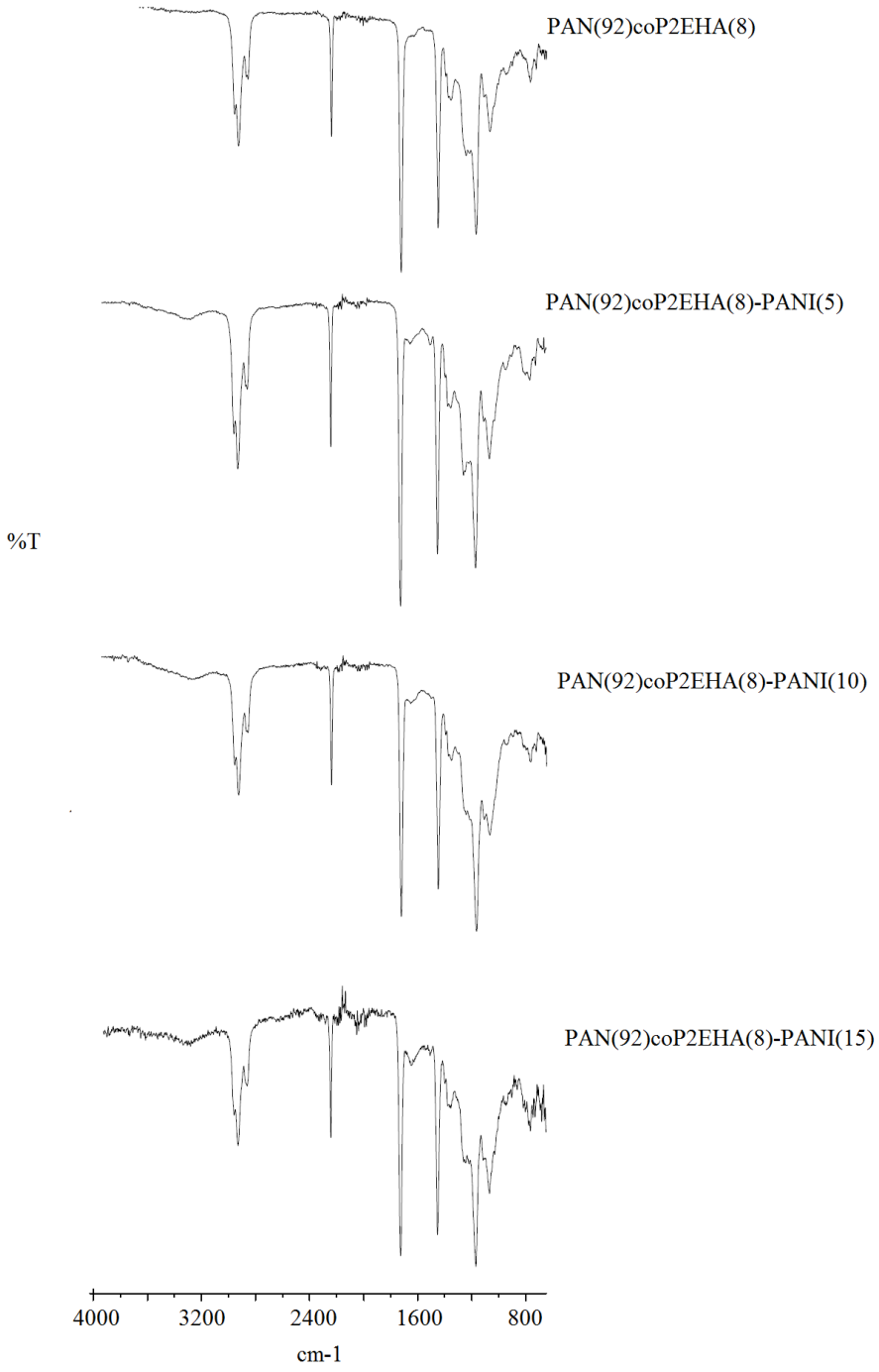

Figure 3.12 FTIR spectroscopy of PAN (92)-co-P2EHA (8) copolymer, PAN (92)-co-P2EHA (8)-PANI (5), PAN (92)-co-P2EHA-PANI (10), PAN (92)-co-P2EHA (8)-PAN (15)

3.3.2 Fracture Morphology of the Nanoporous Filtration Membranes

Fracture morphologies of poly (acrylonitrile (92)-co-2ethylhexyl acrylate (8)) copolymer membrane, poly (acrylonitrile (92)-co-2ethylhexyl acrylate (8)) –PANI (5), poly (acrylonitrile (92)-co-2ethylhexyl acrylate (8))-PANI (10) and poly (acrylonitrile (92)-co-2ethylhexyl acrylate (8))-PANI (15) nanoporous filtration membranes can be seen in Figure 3.13 and fracture morphologies of membranes were comparable . The scanning electron micrographs showed that there was no phase separation in the fracture morphology. The pore sizes of the membranes were also comparable (Figure 3.14).

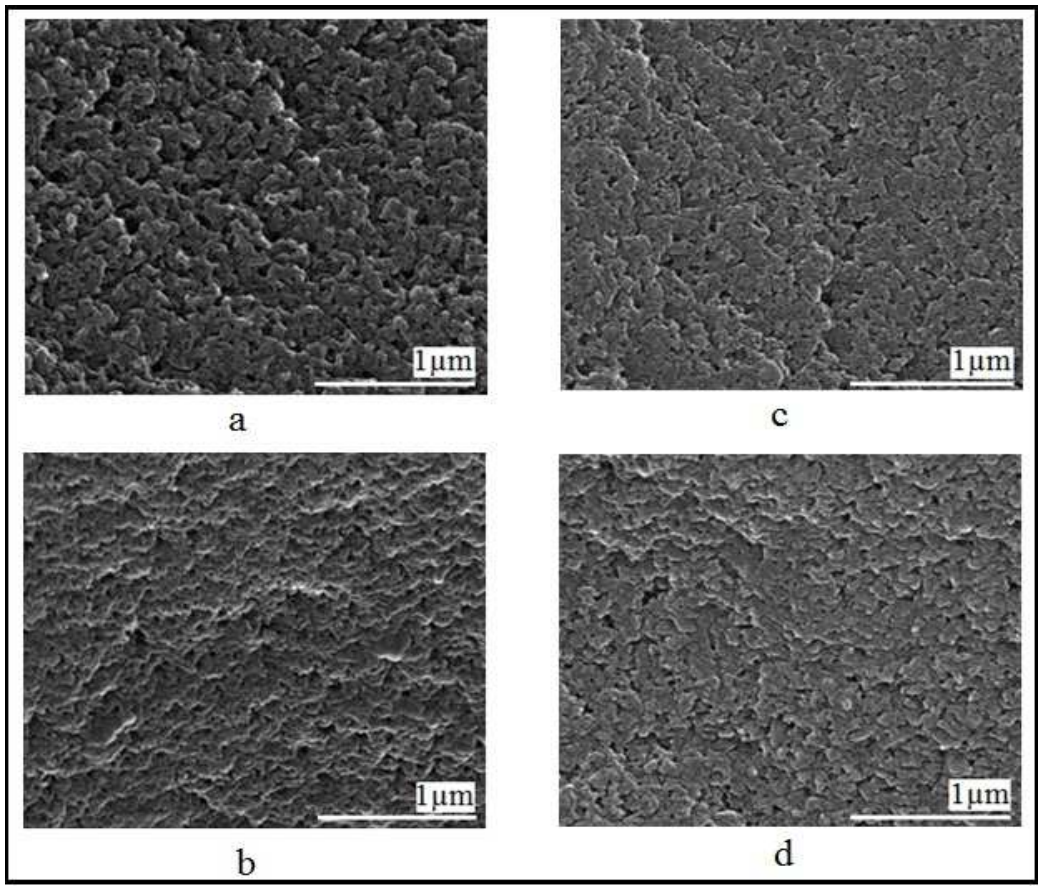

Figure 3.13 Fracture morphology of a. PAN (92)-co-P2EHA (8) b. PAN (92)-co-P2EHA (8)-PANI (5) c. PAN (92)-co-P2EHA (8)-PANI (5) d. PAN (92)-co-P2EHA (8)-PANI (15) membranes

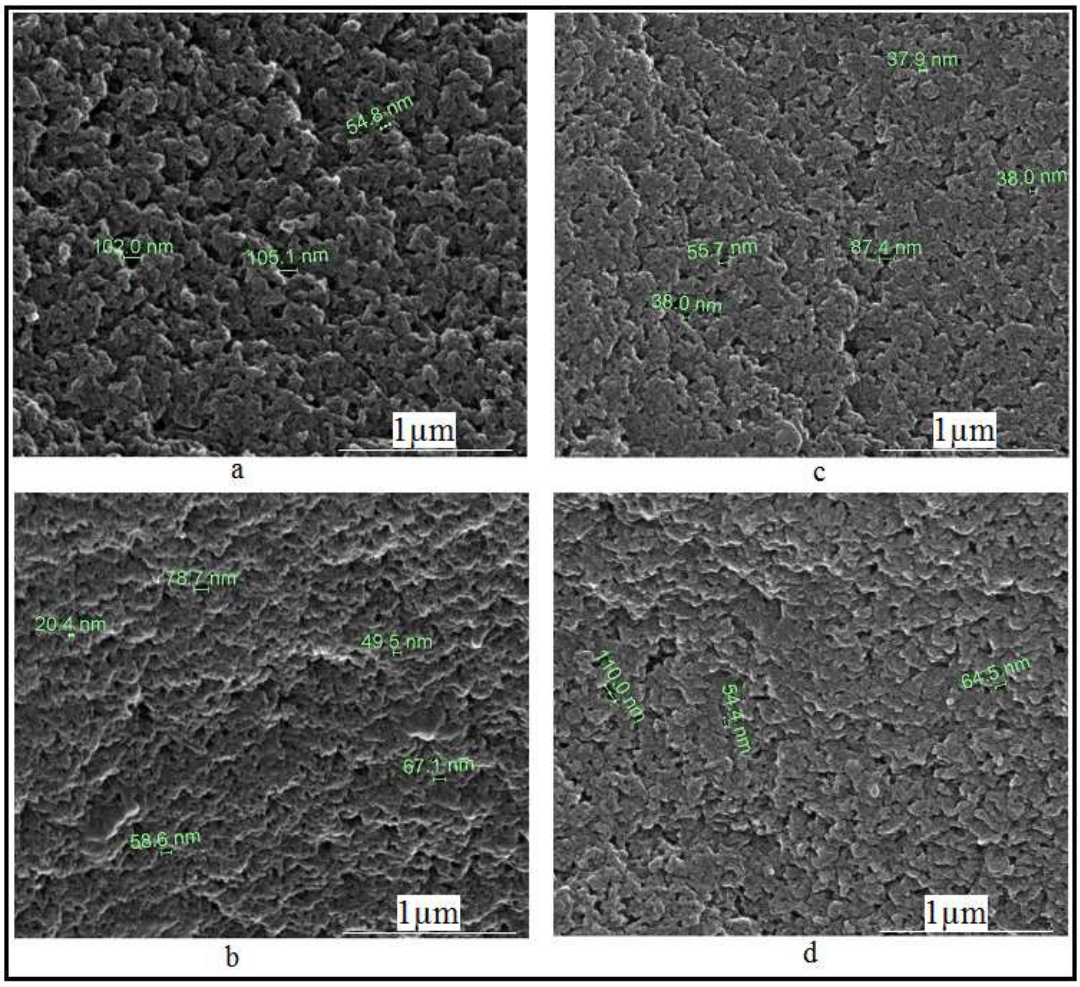

Figure 3.14 Pore size of the membranes a. PAN (92)-co-P2EHA (8) b. PAN (92)-co-P2EHA (8)-PANI (5) c. PAN (92)-co-P2EHA (8)-PANI (5) d. PAN (92)-co-P2EHA (8)-PANI (15) membranes

3.3.3 Swelling and Electrical Properties of the Nanoporous Filtration Membranes

As seen in Table 3.12, the swelling ratio was a function of PANI content. In other words, the swelling characteristics of nanoporous filtration membranes were attributed to PANI, since fracture morphologies of the membranes were almost similar. It is well known that hydrophilicity makes for easier transport water though the membranes. Therefore, the doping process was applied in order to create additional hydrophilicity on the surface of the membranes. Further increase in the

PANI causes the membrane to absorb more water, as seen in the Table3.12, the swelling ratio of the poly (acrylonitrile (92)-co-2ethylhexyl acrylate (8)) – PANI (15) composite membrane were two times greater than that of poly (acrylonitrile (92)-co-2ethylhexyl acrylate (8)) bare copolymer membrane. Additionally, the increase in the PANI content from 5 to 15 percent lead to increase electric conductivities of the membrane, showing that additional protonation was achieved with increase in PANI content.

Table 3.12 Swelling Ratios and Sheet Resistivities of Copolymer and Nanoporous Filtration Membranes

Copolymer and Nanoporous Filtration Membranes	Polyaniline Content (weight percent)	Swelling Ratio (weight percent)	Sheet Resistivity (Ω/sq)
PAN(92)-co-P2EHA(8)	-	2.6	-
PAN(92)-co-P2EHA(8)-PANI(5)	5	5.8	$4.7x10^4$
PAN(92)-co-P2EHA(8)-PANI(10)	10	8.8	$2.0x10^4$
PAN(92)-co-P2EHA(8)-PANI(15)	15	9.2	$4.4x10^3$

3.3.4 Performance of Nanoporous Filtration Membranes Prepared from poly (acrylonitrile (92)-co-2ethylhexyl acrylate (8))

The pure water flux of nanoporous filtration membranes increased as PANI loadings were increased from 5 to 10 and 15 percents (as weight), as seen in the Table 3.13, since the recorded pure water was flux 165 L/m^2h, 175 L/m^2h and 212 L/m^2h respectively. As noted before nanoporous filtration membranes were in

comparable fracture morphology and further addition of PANI made membranes more hydrophilic due to charges created during doping process. This explains the increase in the water flux. It is well known that when water uptake increases, water transport becomes much easier [51, 52]. Permeate flux of nanoporous filtration membranes having three different PANI percentages were shown in Table 3.13. It can be concluded that as chromium (VI) concentration increases, there is a decline in permeate fluxes because of so called concentration polarization which reduces mass transport. Later, chromium removal performances were evaluated by dead end filtration. A 250 ppm chromium (VI) solution was directly passed through membrane with almost no rejection (maximum 1 %) for nanoporous filtration membrane having 5% PANI. This was almost equal to pure copolymer matrix performance without PANI loading. At 50 ppm and 100 ppm chromium (VI) concentrations, permeate flux were ranged from 125 to 155 L/m^2h. One can easily notice that PANI has an influence on both permeate flux and chromium rejection during the filtration. PANI content increased from 5 to 10 and 15 percent to further explore the influence of PANI on membrane performance. Permeate fluxes were increased when the PANI content was increased as in the case of pure water flux (Table 3.13). For nanoporous filtration membranes having 15 percent PANI, permeate fluxes were in between about 142 and 161 L/m^2h at lower concentrations where rejection was always very successful. Additionally, there was an improvement in the chromium (VI) rejection for solutions containing 50 ppm and 100 ppm but there was still almost no chromium (VI) rejection observed for solutions containing 250 ppm Cr (VI). Chromium (VI) removal was successfully achieved at 250 ppm for 15 weight percent PANI containing nanoporous filtration membrane (labeled as poly (acrylonitrile (92)-co-2ethylhexyl acrylate (8)) – PANI (15)) at pH 2). Moreover, membrane having %15 percent PANI have greater permeate fluxes and chromium (VI) rejection for solutions containing 50ppm, 100 ppm and 250 pmm chromium (VI) (Table 3.13). It can be concluded from results that increase in the PANI content increased the permeate fluxes and chromium (VI) rejection. This was because of additional hydrophilicity created during the doping

process. Also, it seems that doped PANI adsorb chromate on the surface of the membrane as well as protons from chromate solution at lower pHs. This will help chromate adsorption on the surface and the water transport through the membrane with higher chromium (VI) rejection.

Table 3.13 Pure Water, Permeate Fluxes and Total Flux Losses of Nanoporous Filtration Membranes at Various Chromium (VI) concentrations and pHs

pH	Cr(VI) (ppm)	Membrane	Pure water flux (L/m^2h)	Permeate Flux (L/m^2h)	Membrane	Pure water flux (L/m^2h)	Permeate Flux (L/m^2h)	Membrane	Pure water flux (L/m^2h)	Permeate Flux (L/m^2h)
2	50	PAN(92)-co-P2-EHA(8)-PAN(5)	165	150	PAN(92)-co-P2EHA(8)-PANI(10)	175	161	PAN(92)-co-P2EHA(8)-PAN(15)	212	177
2	100			132			154			172
2	250			125			135			165
5	50			154			155			199
5	100			148			149			190
5	250			129			132			181

Table 3.13 Continued

pH	Cr(VI) (ppm)	Membrane	Pure water flux (L/m^2h)	Permeate Flux (L/m^2h)	Membrane	Pure water flux (L/m^2h)	Permeate Flux (L/m^2h)	Membrane	Pure water flux (L/m^2h)	Permeate Flux (L/m^2h)
7	50	PAN(92)-co-P2-EHA(8)-PAN(5)	165	155	PAN(92)-co-P2EHA(8)-PANI(10)	175	156	PAN(92)-co-P2EHA(8)-PAN(15)	212	156
7	100			134			142			153
7	250			120			128			149

It can be understood from the results that the chromium (VI) removal from the water is highly pH dependant. Moreover, the hydronium ion has an influence on the chromium rejection because of its adsorbent capacity and effects on the chemical nature of the metal ion. Therefore, the chemical nature of the Cr (VI) ion depends on the pH and concentration of the solution. Cr (VI) is found in different oxy-anion forms such as $Cr_2O_7^{-}$, CrO_4^{2-} and $HCrO_4^{-}$ and H_2CrO_4 depending on pH and the total concentration of the solution (Figure 3.15) [53]. Since experiments were carried out by varying pH of the solutions from pH=2 to pH=7 at three different concentrations (5, 100, 250 ppm) dichromate species is out of focus of this study.

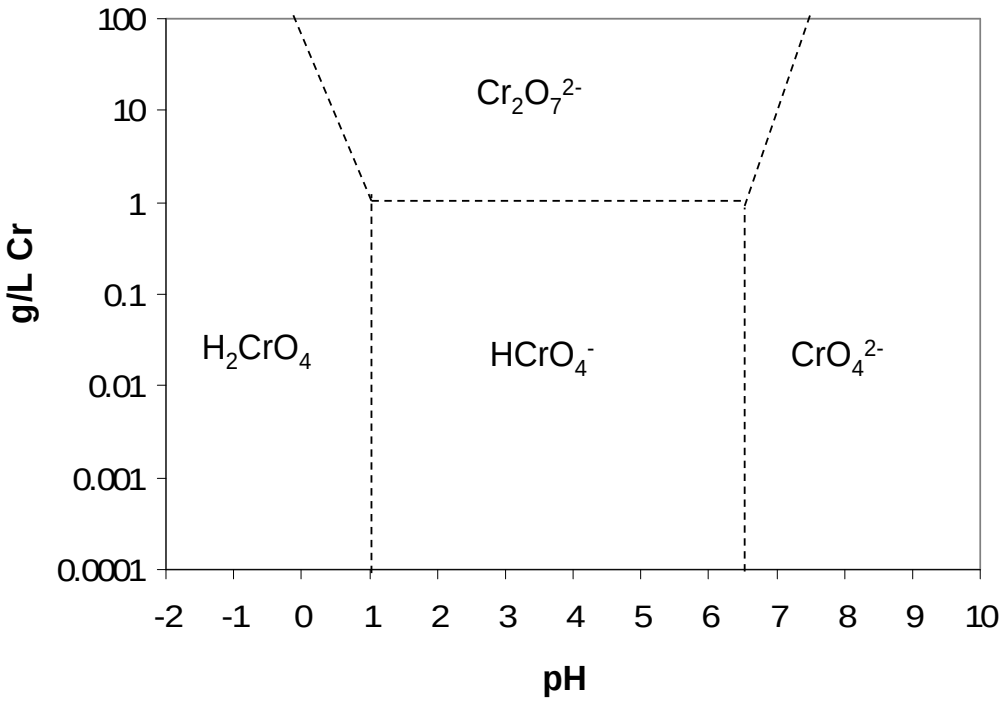

Figure 3.15 Influence of pH and hexavalent chromium concentration on formation of hexavalent chromium species

Since acid treatment made nanoporous filtration membranes positively charged due to its amine protonation, it is estimated that the amine salt functionalized

nanoporous filtration membranes successfully bound the Cr (VI) as monavalent and divalent chromates. This explains the how chromium (VI) rejection successfully achieved with nanoporous filtration membranes, although the fracture morphologies of copolymer and nanoporous filtration membranes comparable. Figure 3.16 shows the percent chromium (VI) removal capability of PAN (92)-co-P2EHA (8)-PANI (5) nanoporous filtration membranes at three different chromium (VI) compositions and various pH values. Maximum rejection of 99.9 % was observed at pH=2 for 50 ppm chromium (VI) solution. At 50 ppm concentration rejection was decreased till about 84.9 % with increasing pH from pH=2 to pH=7. Similar behavior was also observed for 100 ppm solutions. Rejection was high as 95.1 percent at pH=2, but it was reduced to 87.6 % at pH=7. It can be concluded that hydronium ion concentration on the membrane surface decreases with increasing pH causing the decrease in removal of the chromium (VI).

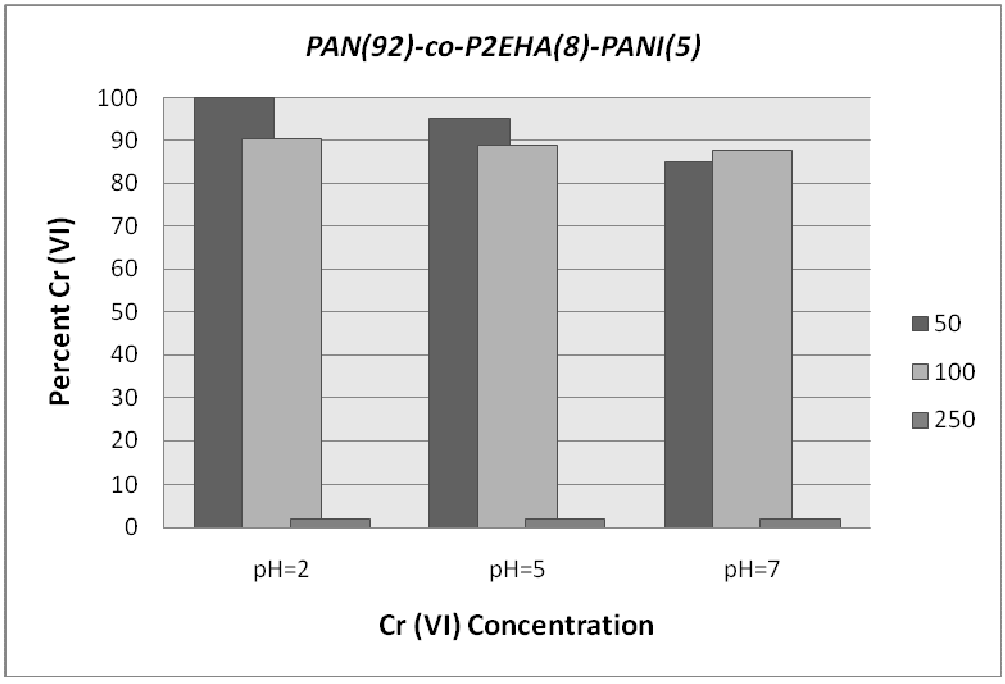

Figure 3.16 Percent chromium removal of PAN (92)-co-P2EHA (8)-PANI (5) nanoporous filtration membranes at various pHs

When the polyaniline weight content was increased from 5 to 10 percent, better performances were observed at pH 5 and pH 7 for the solutions containing 50 ppm and 100 ppm chromium (VI) (Figure 3.17). Better chromium (VI) removals (99.9 %) were observed for the PAN (92)-co-P2EHA (8)-PANI nanoporous filtration membranes having 10 percent PANI loadings at pH 2 for 50 ppm concentrations. At 50 ppm concentration rejection was decreased till about 85.8 % with increasing pH from pH=2 to pH=7. Additionally, the chromium (VI) removal by the PAN (92)-co-P2EHA (8)-PANI (10) nanoporous filtration membranes was almost comparable for solution containing 100 ppm Cr (VI) at various pH. For these membranes having 5 and 10 percent PANI loading, there was almost no chromium (VI) rejection for 250 ppm solutions at three different pHs.

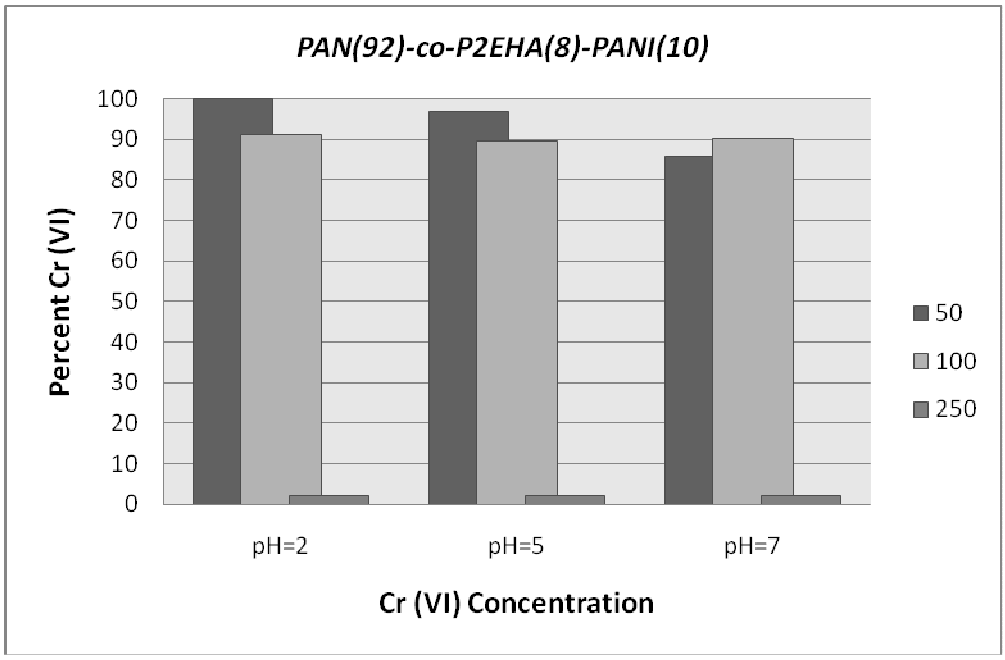

Figure 3.17 Percent chromium removal of PAN (92)-co-P2EHA (8)-PANI (10) nanoporous filtration membranes at various pHs

When polyaniline content further increased from 10 to 15 percent, Cr (VI) rejection at pH 2 for solution containing 250 ppm chromium (VI) was achieved (Figure

3.18). This was possibly due to an increase in the number of positive charges provided by the doped polyaniline which adsorbed more mono and divalent anion on the membrane surface. However, there were still almost no chromium rejections at pH 5 and pH 7. At 50 ppm concentration rejection was decreased from 99. 9 to about 96. 2 % with increasing pH from pH=2 to pH=7. Additionally, the chromium (VI) removal by PAN (92)-co-P2EHA (8)-PANI (15) nanoporous filtration membranes was almost similar for solution containing 100 ppm Cr (VI) at various pH.

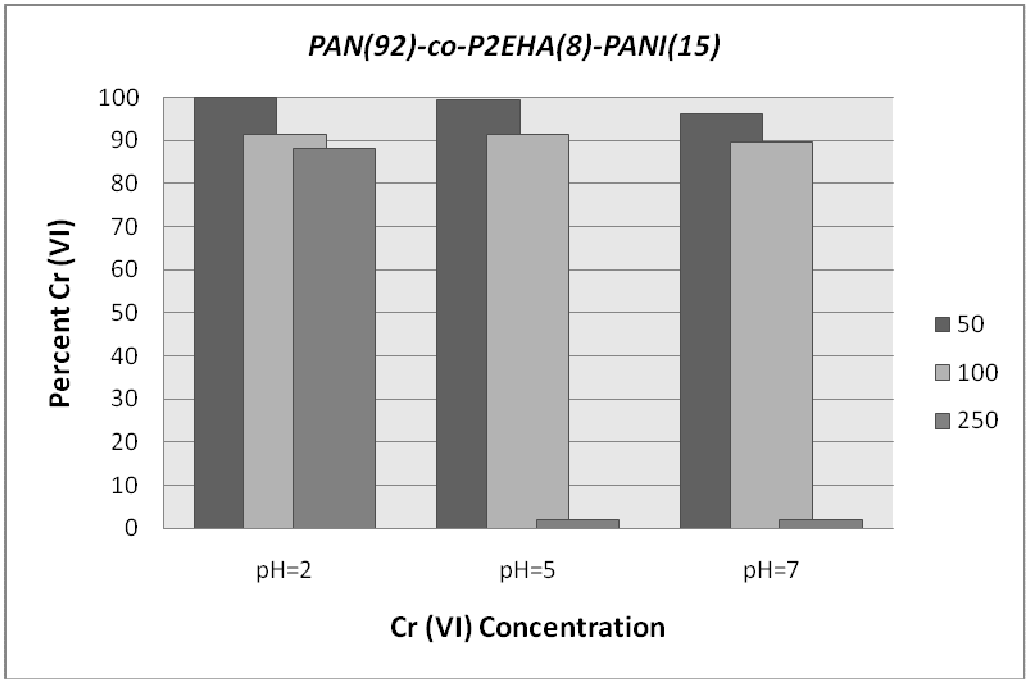

Figure 3.18 Percent chromium removal of PAN (92)-co-P2EHA (8)-PANI (15) nanoporous filtration membranes at various pHs

Since better chromium (VI) removal performances were observed for all three types of nanoporous filtration membrane at pH 2 and 50 ppm containing solutions, fouling analyses were only performed for these membranes at 689.5 kPa for 4h continuous permeation. The data from the fouling analysis were used to calculate

the percent flux loss, total flux loss, reversible and irreversible flux loss [54-56]. It was observed that all nanoporous filtration membranes showed higher flux recovery (greater than 90%) promising better long term performances (Table 3.14). Lower total flux loss number indicates that there were smaller numbers of adsorption on the surface of the nanoporous filtration membranes. Total flux loss includes reversible and irreversible flux losses. Reversible flux loss can easily be removed by water washing of membranes. However, irreversible flux loss is permanent and caused by irreversible deposition of permeate on the membrane active surface. Table 3.14 shows that the total flux loss can be attributed to both reversible flux loss and irreversible flux loss. Reversible and irreversible flux losses were comparable for all samples, i.e, they are almost similar for all three nanoporous filtration membrane. In other words, permanent deposition characteristics of chromium on nanoporous filtration membranes and temporary adsorption on surface were similar.

Table 3.14 Pure Water, Permeate Fluxes and Total Flux Losses of Nanoporous Filtration Membranes after Fouling Test

Types of Nanoporous Filtration Membrane	pH	Cr(VI) (ppm)	Percent flux recovery	Total flux loss	Reversible flux loss	Irreversible flux loss
PAN(92)-co-P2EHA(8)-PAN(5)	2	50	93	0.11	0.044	0.069
PAN(92)-co-P2EHA(8)-PAN(10)	2	50	92	0.11	0.037	0.072
PAN(92)-co-P2EHA(8)-PAN(15)	2	50	92	0.11	0.035	0.073

CHAPTER 4

CONCLUSION

1) Polyacrylonitrile was copolymerized with hexyl acrylate and 2-ethylhexyl acrylate and copolymer of poly (acrylonitrile)-co-2ethylhexyl acrylate) was used in order to prepare nanoporous filtration membranes.

2) Random copolymers of acrylonitrile with hexyl acrylate and 2ethylhexyl acrylate was synthesized by one step emulsion polymerization technique in aqueous medium and FTIR, ^{1}H-NMR was used to clarify their chemical structure. Moreover, From ^{1}H-NMR spectrum, the chemical composition of copolymer was investigated and it was said that comonomers was successfully incorporated into the polymer backbone.

3) TGA results proved that poly (acrylonitrile-co-hexyl acrylate) was thermally stable up to 372 ^{o}C and this was 385 ^{o}C for poly (acrylonitrile-co-2ethylhexyl acrylate).

4) DSC investigations revealed that glass transition temperatures of copolymers differs between the Tg values of homopolymers and an increase in mole percent of comonomer led to the decrease in glass transition temperature of copolymers. The reported glass transition temperatures for polyacrylonitrile and polyhexyl acrylate homopolymers are 103 ^{O}C and -37 ^{O}C respectively and glass transition temperatures of synthesized copolymers were lowered to 68.7 ^{O}C, 56.09 ^{O}C and 52.4 ^{O}C with increasing mole percent of hexyl acrylate incorporated into copolymer from 8 to 12 and 16. The same situation was observed for poly (acrylonitrile-co-2ethylhexyl acrylate) copolymers. The

reported glass transition temperatures for polyacrylonitrile and polyhexyl acrylate homopolymers are 103 ^{O}C and -50 ^{O}C respectively and glass transition temperatures of synthesized copolymers were lowered to 54.7 ^{O}C, 50.04 ^{O}C and 47.3 ^{O}C with increasing mole percents of the hexyl acrylate incorporated into copolymer from 8 to 12 and 16.

5) Thermal analyses of the copolymers were investigated to determine weight loss behavior during successive heating over a period of time. It was observed that the 10 % weight loss temperature increases with increase of molar ratio of hexyl acrylate and 2-ethylhexyl acrylate.

6) Both poly (acrylonitrile-co-hexyl acrylate) and poly (acrylonitrile-co-2ethylhexyl acrylate) copolymer were converted into nanoporous filtration membrane by mixing with PANI and their performance tested with deadend filtration. Results showed that nanoporous filtration membranes prepared with PAN-co-PHA had lower water flux compared to PAN-co-P2EHA so the chromium (VI) removal was achieved by using the nanoporous filtration membranes prepared from poly (acrylonitrile(92)-co-2ethylhexyl acrylate(8)) copolymer with three different PANI loadings (5, 10 and 15 weight percent).

7) Fracture morphologies of the copolymer and nanoporous filtration membranes were studied by SEM.

8) Swelling ratios and electrical conductivity of nanoporous filtration membranes increase with increase of PANI addition.

9) Almost complete chromium removal was achieved at pH 2 for the solution containing 50 ppm chromium with nanoporous filtration membranes having 5, 10 and 15 weight percent PANI. Moreover, approximately 90 % chromium removal was achieved for solution containing 100 ppm chromium at pH 2, 5

and 7 with all types of nanoporous filtration membranes. However, for nanoporous filtration membranes having 5 and 10 percent PANI loading, there was observed almost no chromium (VI) rejection for 250 ppm solutions at three different pH. When polyaniline content further increased from 10 to 15 percent, Cr (VI) rejection at pH 2 for a solution containing 250 ppm chromium (VI) was achieved.

10) Permeate fluxes of the nanoporous filtration membranes range between 125-177 L/m^2h, which indicates that increase in content of PANI from 5 to 10 and 15 weight percent lead to increase both permeate and pure water flux.

11) Porosity sizes of the copolymer and nanoporous filtration membranes were comparable (in the range of 20-110 nm).

12) PANI has a great effect on chromium removal because of the charge created during the acid treatment, making water transport much easier, and the adsorption of mono and the divalent chromium on the membrane surface causing better filtration of chromium (VI).

CHAPTER 5

SUGGESTER FUTURE RESEARCH

1) Production of copolymer with higher molar percent of comonomer.

2) Investigation of effects of amount of initiator, surfactant, and chain transfer agent and temperature on the molecular weight of copolymer and kinetics of polymerization.

3) Examining monomer reactivity ratios of copolymerization system.

4) Examining the thermal degradation behaviors of copolymer by using TGA-FTIR.

5) Investigation of mechanical properties of copolymers and effects of comonomer molar percent on mechanical properties.

6) Utilizing nanoporous filtration membranes for different materials areas.

REFERENCES

1. James F. Bradzil BP, Nitriles Catalysis Research, Acrylonitrile, Kirk-Othmer Encyclopedia of Chemical Technology, John Wiley&Sons Inc.

2. Erich Penzel, Polyacrylates, Ullmann's Encyclopedia of Industrial Chemistry, 2000.

3. Peter A. Lovell, Mohamed S. El-Aasser, Emulsion Polymerization and Emulsion Polymers, John Wiley&Sons Ltd, 5, 9, 10, 14, 34, 38-42, 45-46, 1997.

4. George Odian, Principles of Polymerization Fourth Edition, John Wiley&Sons, Inc., 350, 352, 355-357, 367, 2004.

5. C.S. Chern, Emulsion Polymerization Mechanisim and Kinetics Proggres in Polymer Science, Elseveir, 444-447, 2006.

6. Richar W. Baker, Membrane Technology and Applications 2nd Edition, John Wiley&Sons, Ltd., 1-8, 17, 208 2004.

7. J.S. Vrentas, C.M. Vrentas Transport in nonporous membranes, Chemical Engineering Science 57, 4199 – 4208, 4199, 2002.

8. C.J.M van Rijn Membrane, Science And Technolgy Series 10, Nano and Micro Engineered Membrane Technology, Elsevier B.V 2004.

9. Chang-Soo Jun, Kew-Ho Lee Palladium and palladium alloy composite membranes prepared by metal-organic chemical vapor deposition method (cold-wall) Journal of Membrane Science 176, 121–130, 121, 2000.

10. Raquel Fortunato, Carlos A.M. Afonso, M.A.M. Reis, Joao G. Crespo, Supported liquid membranes using ionic liquids: study of stability and transport mechanism, Journal of Membrane Science 242, 197–209, 197, 2004.

11. Naheed Bukhari, M. Ashraf Chaudrt, M. Mazhar, Cobalt(II) transport through triethanolamine–cyclohexanone supported liquid membranes, Journal of Membrane Science 234,157–165, 157, 2004.

12. Eun-Sik Kima, Young Jo Kimb, Qingsong Yub, Baolin Denga, Preparation and characterization of polyamide thin-film composite (TFC) membranes on plasma-modified polyvinylidene fluoride (PVDF), Journal of Membrane Science 344,71–81, 71, 2009.

13. Marcel Mulder, Basic Principles of Membrane Technology Second Edition, Kluwer Academic Publisher, 7-9, 75-77, 172, 1996.

14. Simon Judd, The MBR Book Principles and Applications of Membrane Bioreactors in Water and Wastewater Treatment, Elsevier Ltd., 30, 2006.

15. Ken Sutherland, Filters and Filtration Handbook Fifth Edition, Elsevier Ltd., 192, 2008.

16. Nicholas P. Cheremisinoff, Handbook of Water and Wastewater Treatment Technologies, Butterworth-Heinemann, 360, 2002.

17. C. Fritzmann, J. Löwenberg, T. Wintgens, T. Melin, State-of-the-art of reverse osmosis desalination, Desalination 216 , 1–76, 8-9, 2007.

18. Manjeet Bansal, Diwan Singh, V.K. Garg, A comparative study for the removal of hexavalent chromium from aqueous solution by agriculture wastes' carbons, Journal of Hazardous Materials 171, 83–92, 83, 2009.

19. Violeta Neagu, Removal of Cr(VI) onto functionalized pyridine copolymer with amide groups, Journal of Hazardous Materials 171 ,410–416, 410, 2009.

20. J.L. Gardea-Torresdey, K.J. Tiemann, V. Armendariz, L. Bess-Oberto, R.R. Chianelli, J. Rios, J.G. Parsons, G. Gamez, Characterization of Cr(VI) binding and reduction to Cr(III) by the agricultural byproducts of Avena monida (Oat) biomass, Journal of Hazardous Materials B80 ,175–188, 175, 176, 2000.

21. EPA, Environmental Protection Agency, Environmental Pollution Control Alternatives, EPA/625/5-90/025, EPA/625/4-89/023, Cincinnati, US, 1990.

22. Turkish Standard Institution, Water intended for human consumption TS-266.

23. G. Almaguer-Busso, G. Velasco-Martínez, G. Carreño-Aguilera, S. Gutiérrez-Granados, E. Torres-Reyes, A. Alatorre-Ordaz, A comparative study of global hexavalent chromium removal by chemical and

electrochemical processes, Electrochemistry Communications 11 ,1097–1100, 2009.

24. A.K. Golder, A.N. Samanta, S. Ray, Removal of Cr^{3+} by electrocoagulation with multiple electrodes: Bipolar and monopolar configurations, Journal of Hazardous Materials 141,653–661, 2007.

25. LI Che, LAN Ye-Qing, DENG Bao-Lin Catalysis of Manganese(I1) on Chromium(V1), Pedosphere 17(3):,318-323, 2007.

26. Rifaqat A.K., Rao Fouzia Rehman, Adsorption studies on fruits of Gular (Ficus glomerata): Removal of Cr(VI) from synthetic wastewater, Journal of Hazardous Materials 181 , 405–412, 2010-10-26.

27. P. Venkateswaran, K. Palanivelu, Solvent extraction of hexavalent chromium with tetrabutyl ammonium bromide from aqueous solution, Separation and Purification Technology 40 ,279–284, 2004.

28. G. Cetinkaya Donmez, Z. Aksu, A. Ozturk, A comparative study on heavy metal biosorption characteristics of some algae, Process Biochemistry 34, 885–892, 1999.

29. Guven Ozdemir, Nur Ceyhan, Tansel Ozturk, Feyza Akirmak, Tamer Cosar, Biosorption of chromium(VI), cadmium(II) and copper(II) by Pantoea sp. TEM18, Chemical Engineering Journal 102 , 249–253, 2004.

30. Gonul Donmez, Zumriye Aksu, Removal of chromium(VI) from saline wastewaters by Dunaliella species, Process Biochemistry 38 ,751/762, 2002.

31. G. Tiravanti, D. Petruzzelli, R. Passiono, Pretreatment of tannery wastewaters by an ion exchange process for Cr(III) removal and recovery,Water Sci. Technol. 36, 197–207, 1997.

32. N.F Fahim, B.N Barsoum, A. E Eid, M.S Kahalil, Removal of chromium(III) from tannery wastewater using activated carbon from sugar industrial waste, Journal of Hazardous Materials B136 ,303–309, 2006.

33. Lior Boguslavsky, Sigal Baruch, Shlomo Margel, Synthesis and Characterization of polyacrylonitrile nanoparticles by dispersion/emulsion polymerization process, Journal of Colloid and Interface Science 289, 71-75, 2005.

34. Katharina Landfester, Markus Antonietti, The polymerization of acrylonitrile in miniemulsions: “Crumpled latex particles” or polymer nanocrystals, Macromol. Rapid Commun. 21, 820–824, 2000.

35. T. Jeevananda, Siddaramaiah, S. Seetharamu, S. Saravanan, Lawrence D'Souza, Synthesis and characterization of poly (aniline-co-acrylonitrile) using organic benzoyl peroxide by inverted emulsion method, Synthetic Metals 140, 247-260, 2004.

36. Chen Zhanga, Zhongjie Dua, Hangquan Li, Eli Ruckenstein, High-rate polymerization of acrylonitrile and butyl acrylate based on a concentrated emulsion, Polymer 43, 5391–5396, 2002.

37. Zheng Tian, Xiangming He, Weihua Pu, Chunrong Wan, Changyin Jiang Preparation of poly(acrylonitrile–butyl acrylate) gel electrolyte for lithium-ion batteries, Electrochimica Acta 52 , 688–693, 2002.

38. Chen Zhanga, Zhongjie Dua, Hangquan Li, Eli Ruckenstein, Acrylonitrile-co-vinyl acetate with uniform composition via adiabatic self-healing copolymerization in a concentrated emulsion, Polymer 43, 2945-2951, 2002.

39. Nico Schamag, Heinz Buschatz, Polyacrylonitrile (PAN) membranes for ultra and microfiltration, Desalination 139 , 191-198, 2001.

40. K. Nouzaki, M. Nagata, J. Arai, Y. Idemoto, N. Koura, H. Yanagishita, H. Negishi, D. Kitamoto, T. Ikegami, K. Haraya, Preparation of

polyacrylonitrile ultrafiltration membranes for wastewater treatment, Desalination 144, 53-59, 2002.

41. Sonny Sachdeva, Anil Kumar, Synthesis and modeling of composite poly (styrene-co-acrylonitrile) membrane for the separation of chromic acid, Journal of Membrane Science 307 , 37–52, 2008.

42. Jinwen Wang, Zhongren Yue, Jeffrey Scott Ince, James Economy Preparation of nanofiltration membranes from polyacrylonitrile ultrafiltration membranes, Journal of Membrane Science 286 , 333–341, 2006.

43. Kris R.M. Vidts, Bart Dervaux, Filip E. Du Prez, Block, blocky gradient and random copolymers of 2-ethylhexyl acrylate and acrylic acid by atom transfer radical polymerization, Polymer 47 , 6028-6037, 2006.

44. Amir H. Shojaei, Jennifer Paulson, Sohayla Honary, Evaluation of poly(acrylic acid-co-ethylhexyl acrylate) films for mucoadhesive transbuccal drug delivery: factors affecting the force of mucoadhesion, Journal of Controlled Release 67 , 223–232, 2000.

45. Gabriela E Fonseca, Timothy F. L. McKenna, Marc A. Dube, Preparation of Stable Miniemulsions of Poly (2-ethylhexyl acrylate-co-vinyl acrylate), Macromol. Symp., 72-85, 2010.

46. G. Pratap, K. L. Shantha, D. V. Mohan Rao, V. S. Bhaskar Rao, Synthesis, Chracterization and Evaluation of poly (n-alkyl (oxy)-n-hexyl acrylates), Journal of App. Polymer Science, Vol. 42, 935-945, 1991.

47. Haimanti Datta, Nikhil K. Singha, Atom Transfer Radical Polymerization of Hexyl Acrylate and Preparation of its "All-acrylate" Block Copolymer, Journal of Polymer Science Part A: Polymer Chemistry, Vol. 46, 3499-3511, 2008.

48. L.S. Cleseri, A.E. Greenberg, R.R. Trusells, (Eds.), Standard Methods for the Examination of Water and Wastewater, 17th ed., American Public Health Association, Washington, 1989.

49. Tonelli, A. E., Glass Transition Temperatures of Regularly Alternating Acrylonitrile-Vinyl Acetate Copolymers, Macromolecules, 10(3), 716-717, 1977.

50. Wanqiang Liu, Chenzhong Cao, Artificial neural network prediction of glass transition temperature of polymers, Colloid Polym Sci, 287:811–818, 2009.

51. F.D.R. Amado, M.A.S. Rodrigues, D.A. Bertuol, A.M. Bernardes, J.Z. Ferreira, C.A. Ferreira, J. Membr. Sci. 330, 227–232, 2009.

52. M. Sankir, Y.S. Kim, B.S. Pivovar, J.E. McGrath, J. Membrane. Sci. 299, 8–18, 2007.

53. S.S. Chen, B.C. Hsu, C.H. Ko, P.C. Chuang, Desalination 229, 147-155, 2008.

54. G. Arthanareeswaran, T.K. Sriyamuna, D.D. Mohan; Sep. Purif. Technol. 67, 271-281, 2009.

55. A. Rahimpour, S.S. Madaeni, M. Amirinejad, Y.Mansourpanah, S. Zereshki; J. Membr. Sci. 330, 189–204, 2009.

56. Y.L. Su; W. Cheng; C. Li; Z. Jiang; J. Membr. Sci. 329, 246–252, 2009.